Processing report

Company	**Conoco Phillips**
Project	**Chinook**
Well	**Loon Creek O-06**
Area	**Chinook**
Survey Type	**Zero Offset and Walk-away VSP**
Survey Date	**27 February 2013**
Processing Date	**April 2013**
Prepared by	**Sorin Dobrovicescu, Richard Pearcy**
Job reference ID	**201303**

RESERVOIR IMAGING

ConocoPhillips Canada

Contents

Recorded survey

The purpose of the survey was to collect a Zero Offset and a Walk-away VSP. An array of 122 tri-component down-hole geophones with 15.04m spacing was used. The array covered the whole well.

Top Geophone (m from GL)	**Bottom Geophone (m from GL)**
0.66	1820.5

Acquisition parameters

Seismic source – Vibroseis
No of sweeps/source position – 8
Recording – 1ms sample rate; SEGD format; Recording length 22s (16s sweep + 6s listen time)
Sweep: 16sec length, 8-120Hz linear, 0.3s cosine tapers
Receivers: 122 level 3C DS150 geophones @ 15.04m
Pre Amp Gain: 42dB

Survey geometry (NAD 83) Zone 9

Point	Well	Zero Offset
Easting (m)	593469.49	593639.99
Northing (m)	7220814.46	7221171.03
Elevation (m) (GL)	252.40	247.47

Zero Offset VSP processing

A true zero offset VSP (11m away from the wellhead - Figure 1) was recorded. Data recorded from this position had a very strong tube-wave and was not used further in the zero offset processing. The first arrivals were used to obtain a time-depth table (Figure 2) – seismic datum at KB (257.6m) replacement velocity 3200m/s – a 5 traces (mean) smoothing operator (sliding window) was used for the interval velocity smoothing.

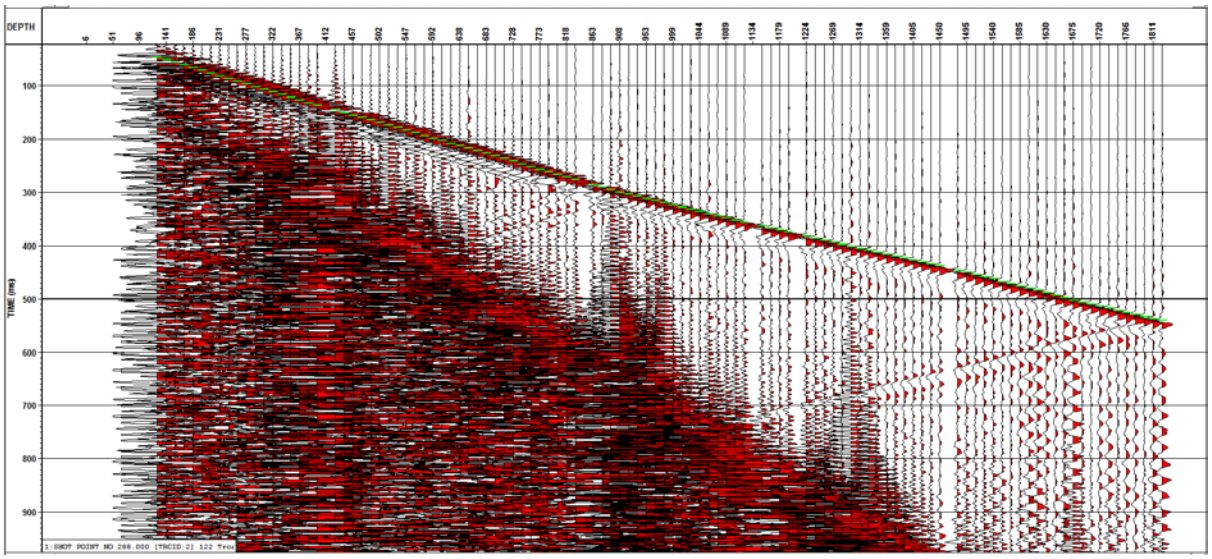

Figure 1 True zero offset - vertical component

MD_Depth	One_Way_Time	P_Interval_Vel
171.30	60.95	
186.34	66.05	2948.15
201.38	71.34	2841.23
216.42	76.55	2886.12
231.46	81.78	2875.70
246.50	86.94	2915.33
261.54	92.10	2914.41
276.58	97.36	2862.14
291.62	102.46	2949.10
306.66	107.48	2994.47
321.70	112.45	3027.97
336.74	117.40	3034.95
351.78	122.36	3034.67
366.82	127.39	2991.56
381.86	132.07	3210.93
396.90	136.85	3145.15
426.98	146.31	3179.44
442.02	150.98	3225.62

457.06	155.96	3018.11
472.10	160.78	3118.56
487.14	165.46	3215.81
502.18	170.18	3188.41
517.22	174.88	3197.13
532.26	179.66	3146.53
547.30	184.46	3137.01
562.34	189.25	3137.46
577.38	194.03	3148.90
592.42	198.86	3112.69
607.46	203.60	3171.17
622.50	208.33	3180.90
637.54	213.14	3127.97
652.58	217.97	3114.53
667.62	222.75	3142.51
682.66	227.64	3078.93
697.70	232.59	3033.24
712.74	237.53	3048.76
727.78	242.51	3020.00
742.82	247.53	2996.12
757.86	252.41	3083.70
772.90	257.28	3083.47
787.94	262.08	3132.08
802.98	266.80	3189.75
818.02	271.62	3122.68
833.06	276.37	3160.77
863.14	285.76	3203.70
878.18	290.63	3092.38
893.22	295.10	3365.10
908.26	299.57	3360.86
923.30	303.99	3402.14
938.34	308.19	3581.45
953.38	312.20	3752.07
968.42	316.31	3658.21
983.46	320.36	3712.40
998.50	324.39	3738.80
1013.54	328.48	3677.71
1028.58	332.48	3754.66
1043.62	336.48	3762.42
1058.66	340.52	3717.78
1073.70	344.50	3781.47
1088.74	348.41	3848.54

1103.78	352.32	3850.19
1118.82	356.19	3880.69
1148.90	363.88	3914.52
1163.94	367.83	3802.75
1178.98	371.60	3992.84
1194.02	375.24	4131.34
1224.10	382.75	4001.98
1239.14	386.56	3949.29
1254.18	390.55	3771.43
1269.22	393.95	4427.56
1284.26	397.78	3923.26
1299.30	401.42	4134.57
1314.34	405.08	4103.72
1329.38	408.77	4080.17
1344.42	412.37	4171.91
1359.46	416.12	4018.85
1374.50	419.86	4022.76
1389.54	423.63	3988.51
1404.58	427.39	4000.58
1419.62	431.15	3992.39
1434.66	434.88	4039.44
1449.70	438.77	3866.23
1479.78	446.79	3747.56
1494.82	450.89	3669.17
1509.86	455.08	3590.71
1524.90	459.19	3661.67
1539.94	463.30	3654.13
1554.98	467.43	3640.79
1570.02	471.55	3657.81
1585.06	475.69	3630.55
1600.10	479.89	3581.08
1615.14	484.18	3503.94
1630.18	488.58	3420.85
1645.22	493.12	3309.31
1660.26	497.60	3356.59
1675.30	501.97	3443.94
1690.34	506.18	3572.20
1705.38	510.21	3729.79
1720.42	514.12	3851.57
1735.46	517.99	3886.44
1750.50	521.92	3823.07
1765.54	525.89	3789.73

1780.58	529.92	3734.82
1795.62	533.90	3776.61
1810.66	537.75	3908.02
1825.70	540.07	6487.53

Figure 2 Time - depth table and interval velocity

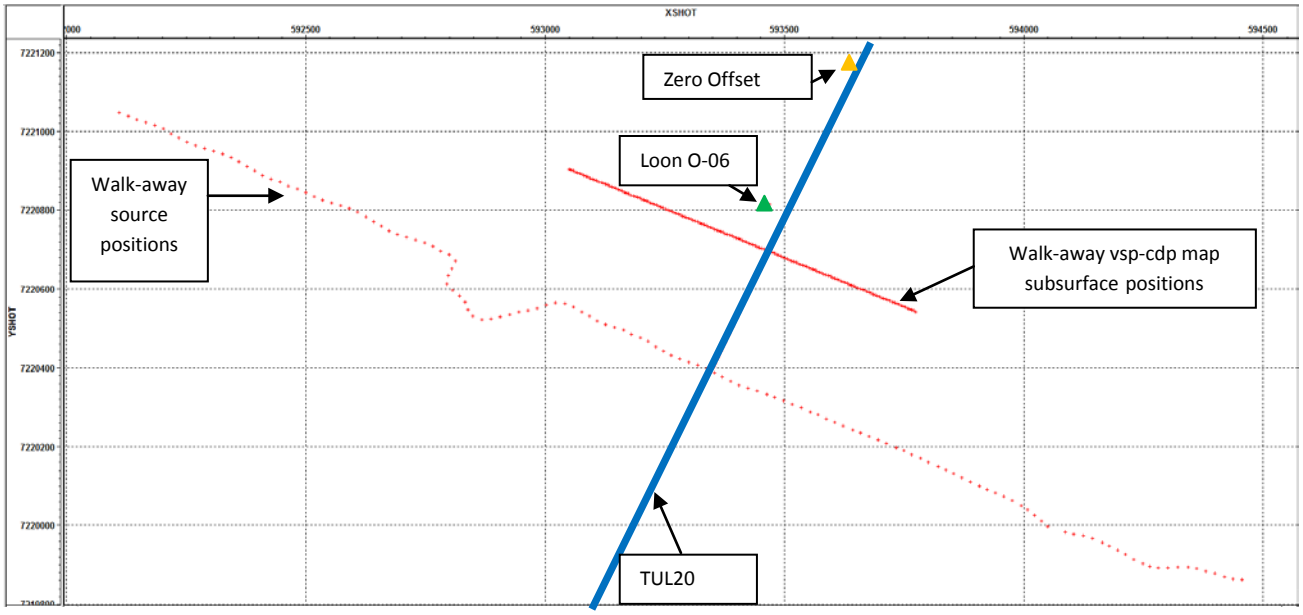

Figure 3 Basemap

Another shot-point was used for the zero offset processing (Figure 3) that was at 395m away from the wellhead.

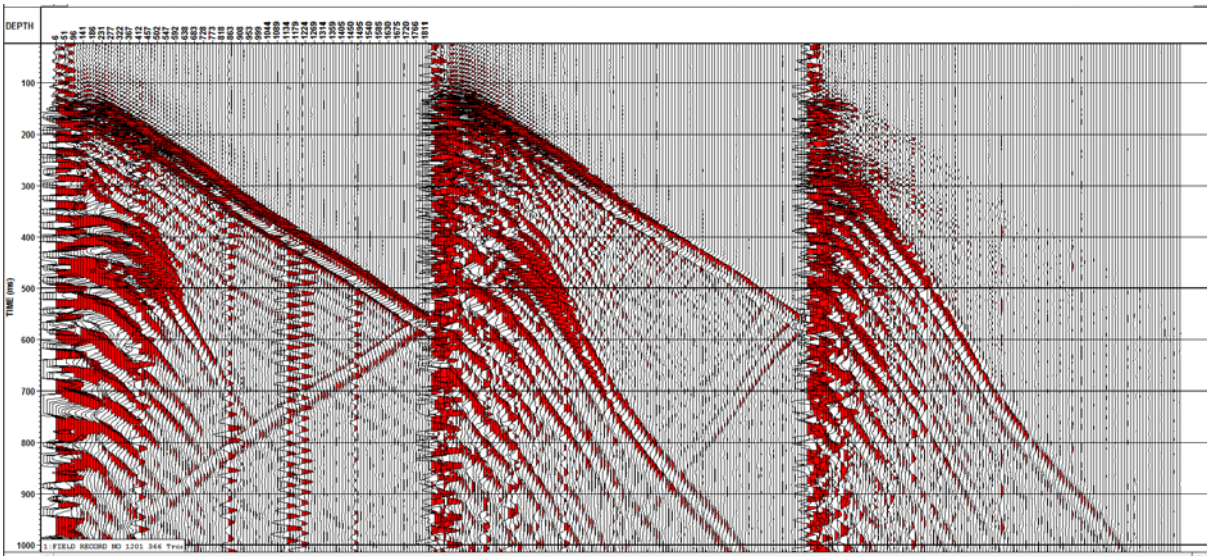

Figure 4 Zero offset raw data - vertical (left) Hmax (middle) and Hmin (right)

Data quality is very good with the exception of 5 levels on the vertical component. For the zero offset processing only the vertical component was used.

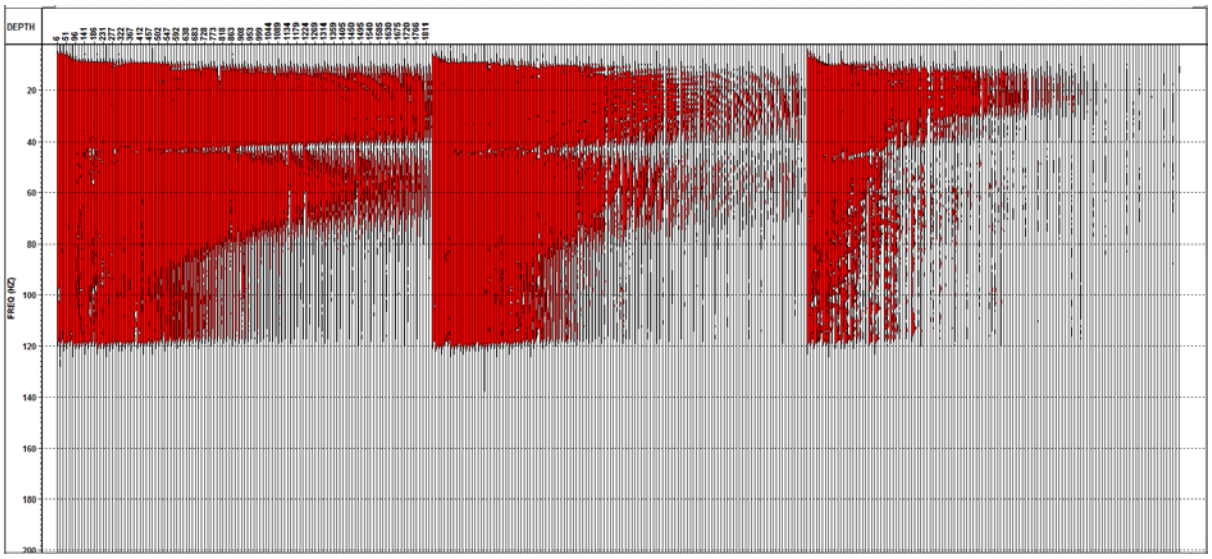

Figure 5 Amplitude spectrums of data shown in Figure 4

The first 6-7 levels are in a zone with bad/no cementation.

Processing steps – vertical component

Step 1 – Geometry – source and well coordinates, well deviation, receiver depths were applied to the data. Seismic datum was chosen 257.6m (KB). Replacement velocity was 3200m/s

Step 2 – Amplitude correction – A spherical divergence correction (T power 1.5) was applied

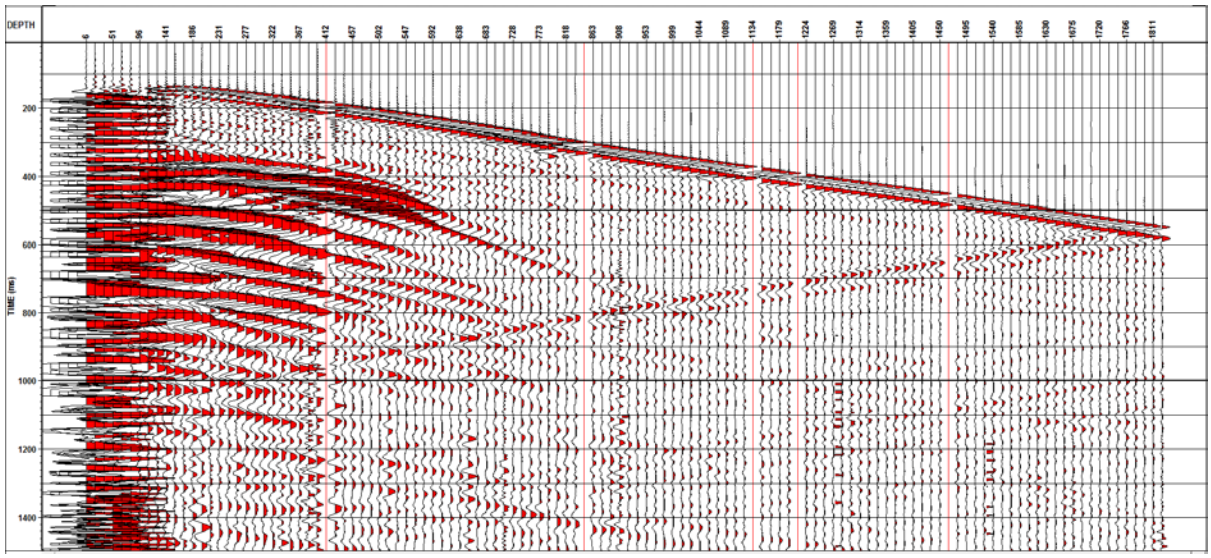

Figure 6 Raw data after amplitude correction - vertical component

Step 3 – First arrivals pick and interval velocity calculation – First arrivals were picked on the data and interval velocities were calculated. Due to data quality both P and S could be picked.

Below are shown the P and S arrival times and interval velocities in both graphic and table form. A 5 traces (mean) smoothing operator (sliding window) was used to smooth the S velocities.

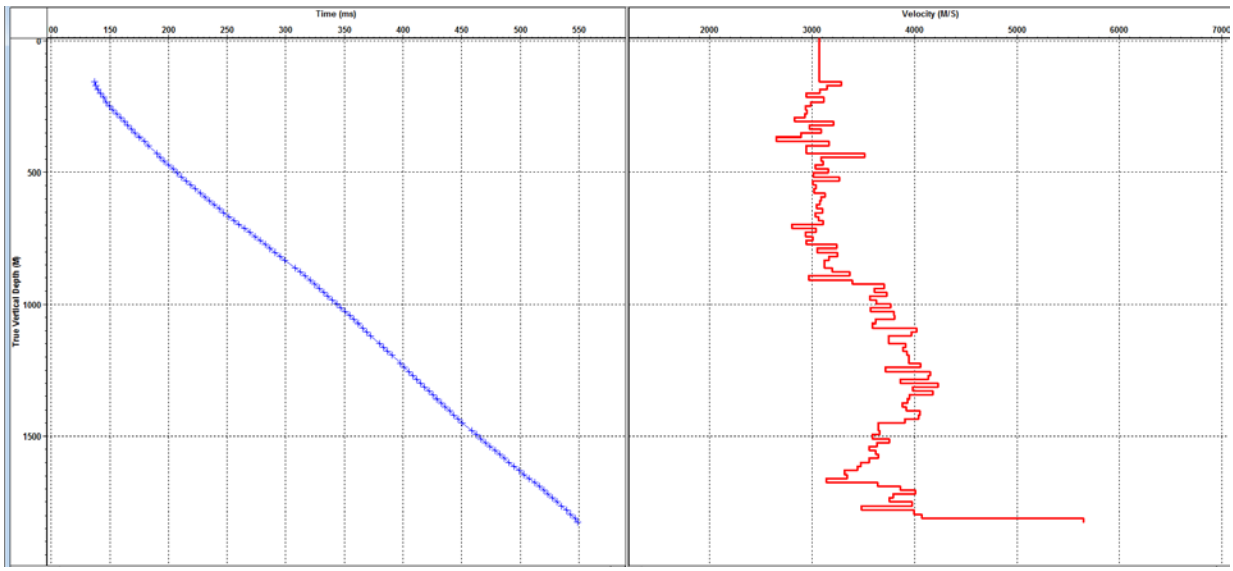

Figure 7 P travel times and calculated interval velocity

MD_Depth	One_Way_P_Time	P_Interval_Vel
156.26	47.58	
171.30	52.16	3282.10
186.34	56.94	3145.41
201.38	61.84	3072.68
216.42	66.95	2940.73
231.46	71.79	3112.90
246.50	76.83	2983.31
261.54	81.96	2932.68
276.58	87.05	2949.90
291.62	92.19	2927.19
306.66	97.51	2826.13
321.70	102.20	3208.23
336.74	107.26	2971.23
351.78	112.13	3088.62
366.82	117.34	2890.41
381.86	123.01	2648.58
396.90	127.77	3164.96
426.98	137.99	2941.76

442.02	142.28	3509.10
457.06	147.15	3088.74
472.10	151.99	3108.04
487.14	156.95	3029.70
502.18	161.72	3155.59
517.22	166.71	3012.76
532.26	171.31	3267.56
547.30	176.32	3002.25
562.34	181.27	3039.19
577.38	186.25	3017.25
592.42	191.07	3123.36
607.46	195.94	3090.06
622.50	200.83	3073.50
637.54	205.77	3042.07
652.58	210.63	3100.56
667.62	215.59	3029.74
682.66	220.50	3063.74
697.70	225.34	3107.26
712.74	230.71	2801.49
727.78	235.66	3034.63
742.82	240.78	2938.30
757.86	245.79	3005.26
772.90	250.89	2944.68
787.94	255.53	3242.48
802.98	260.47	3046.66
818.02	265.11	3243.86
833.06	269.86	3164.20
863.14	279.49	3122.32
878.18	284.20	3195.19
893.22	288.67	3367.79
908.26	293.73	2967.21
923.30	298.17	3390.08
938.34	302.23	3701.86
953.38	306.40	3607.52
968.42	310.43	3730.82
983.46	314.65	3565.92
998.50	318.80	3627.80
1013.54	322.79	3764.40
1028.58	327.01	3568.06
1043.62	330.97	3795.66
1058.66	334.92	3803.39
1073.70	339.08	3618.31

1088.74	343.27	3590.24
1103.78	347.01	4019.05
1118.82	350.80	3969.55
1148.90	358.82	3749.94
1163.94	362.67	3914.07
1178.98	366.54	3886.50
1194.02	370.37	3921.67
1224.10	378.00	3943.60
1239.14	381.71	4056.83
1254.18	385.76	3713.15
1269.22	389.38	4150.09
1284.26	393.02	4132.07
1299.30	396.92	3857.93
1314.34	400.47	4231.41
1329.38	404.25	3981.07
1344.42	407.85	4179.20
1359.46	411.65	3952.30
1374.50	415.48	3928.58
1389.54	419.36	3882.58
1404.58	423.19	3918.27
1419.62	426.91	4052.50
1434.66	430.63	4035.27
1449.70	434.48	3908.45
1479.78	442.74	3642.27
1494.82	446.85	3655.94
1509.86	451.05	3587.47
1524.90	455.05	3755.68
1539.94	459.19	3635.23
1554.98	463.42	3553.76
1570.02	467.57	3622.46
1585.06	471.70	3644.59
1600.10	475.93	3558.66
1615.14	480.25	3475.96
1630.18	484.62	3445.05
1645.22	489.16	3313.87
1660.26	493.66	3339.88
1675.30	498.45	3140.17
1690.34	502.58	3637.43
1705.38	506.48	3858.36
1720.42	510.23	4007.16
1735.46	514.20	3793.96
1750.50	518.21	3752.74

1765.54	521.99	3973.71
1780.58	526.31	3480.35
1795.62	530.08	3991.12
1810.66	533.78	4067.98
1825.70	536.44	5650.19

Figure 8 P travel times and calculated interval velocity

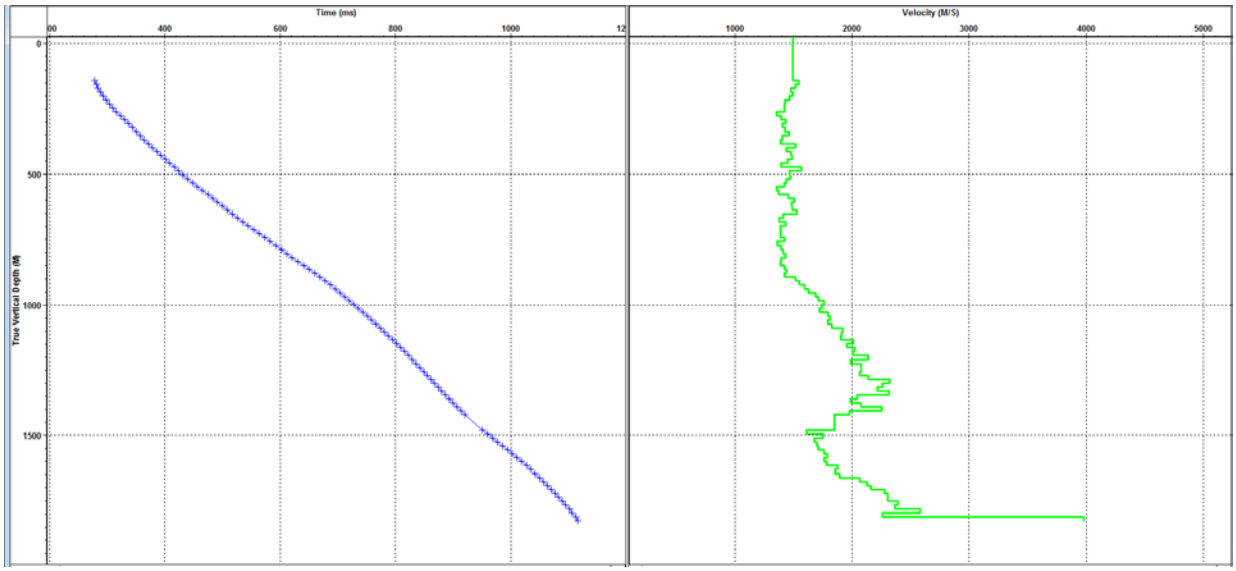

Figure 9 Smoothed S travel times and calculated interval velocity

MD_Depth	One_Way_S_Time	S_Interval_Vel
141.22	87.73	
156.26	97.46	1546.88
171.30	107.37	1517.24
186.34	117.53	1479.98
201.38	127.58	1497.18
216.42	137.83	1466.08
231.46	148.36	1428.25
246.50	158.93	1424.23
261.54	169.49	1423.73
276.58	180.58	1355.70
291.62	191.37	1394.10
306.66	201.84	1436.00
321.70	212.52	1409.11
336.74	223.05	1427.95
351.78	233.35	1460.26
366.82	244.03	1407.67
381.86	254.84	1392.50

396.90	264.73	1519.49
411.94	275.18	1439.87
426.98	285.33	1480.96
442.02	295.41	1491.95
457.06	305.79	1449.22
472.10	316.57	1396.16
487.14	326.15	1569.74
502.18	336.38	1470.15
517.22	346.57	1475.12
532.26	357.00	1442.45
547.30	367.55	1425.42
562.34	378.63	1357.52
577.38	389.59	1372.66
592.42	399.92	1455.63
607.46	409.92	1504.15
622.50	420.06	1483.18
637.54	430.15	1491.02
652.58	440.00	1526.34
667.62	450.64	1412.97
682.66	461.53	1381.15
697.70	472.01	1436.02
712.74	482.83	1389.64
727.78	493.65	1389.84
742.82	504.47	1390.36
757.86	515.03	1424.47
772.90	526.07	1361.41
787.94	536.85	1395.91
802.98	547.48	1415.00
818.02	557.97	1433.46
833.06	568.73	1397.03
848.10	579.57	1387.99
863.14	590.14	1423.23
878.18	600.59	1439.21
893.22	611.14	1425.42
908.26	621.06	1516.22
923.30	630.76	1550.51
938.34	640.18	1596.23
953.38	649.40	1631.22
968.42	658.31	1687.58
983.46	667.11	1710.63
998.50	675.64	1761.78
1013.54	684.25	1747.05

1028.58	692.97	1724.21
1043.62	701.36	1793.89
1058.66	709.67	1809.78
1073.70	718.04	1796.87
1088.74	726.27	1826.30
1103.78	734.11	1920.37
1118.82	741.98	1908.71
1133.86	749.87	1906.45
1148.90	757.34	2013.66
1163.94	765.04	1953.74
1178.98	772.48	2022.92
1194.02	779.99	2002.78
1209.06	787.02	2138.51
1224.10	794.59	1987.11
1239.14	801.82	2078.71
1254.18	809.05	2079.97
1269.22	816.33	2066.87
1284.26	823.36	2138.30
1299.30	829.84	2321.68
1314.34	836.49	2262.09
1329.38	843.28	2213.60
1344.42	849.77	2317.77
1359.46	857.13	2043.84
1374.50	864.70	1987.72
1389.54	871.93	2079.30
1404.58	878.60	2256.56
1419.62	886.19	1979.61
1479.78	918.70	1851.01
1494.82	928.04	1610.10
1509.86	936.63	1751.11
1524.90	945.60	1675.73
1539.94	954.45	1699.57
1554.98	963.25	1709.67
1570.02	971.79	1759.72
1585.06	980.19	1791.20
1600.10	988.73	1760.66
1615.14	997.16	1784.08
1630.18	1005.17	1878.23
1645.22	1013.28	1854.45
1660.26	1021.23	1892.94
1675.30	1028.50	2067.42
1690.34	1035.57	2127.39

1705.38	1042.54	2158.89
1720.42	1049.14	2276.55
1735.46	1055.67	2303.99
1750.50	1062.19	2307.09
1765.54	1068.48	2392.09
1780.58	1074.83	2366.06
1795.62	1080.66	2581.41
1810.66	1087.32	2258.77
1825.70	1091.10	3980.10

Figure 10 Smoothed S travel times and calculated interval velocity

Step 4 – Sonic log calibration – When we want to use sonic log velocities for seismic purposes we need to adjust them to match with seismic measurements. If we calculate the integrated transit time based on the sonic log velocities with depth (the depth – one way travel time curve shown in Figure 11 on the left as a red curve) and we compare those transit times with the same curve derived from the VSP direct arrival times (Figure 11-left-blue curve) we can see that there is a difference between them, mostly due to a higher frequency measurement in the sonic. This difference is called drift (Figure 11-middle – drift curve).

To correct the integrated transit time of the sonic to match the seismic times we are adjusting the sonic velocities so that integrated transit time curves tie. In terms of sonic logs (expressed in slowness - ms/m) this means to correct with the slope of the drift curve (expressed in slowness - ms/m).

The result of the correction is presented in Figure 12 – now the integrated transit time is the same as the time from the VSP and the interval velocities (Figure 12 – right – red curve) are closer to those calculated from the VSP (Figure 12 – right – blue curve).

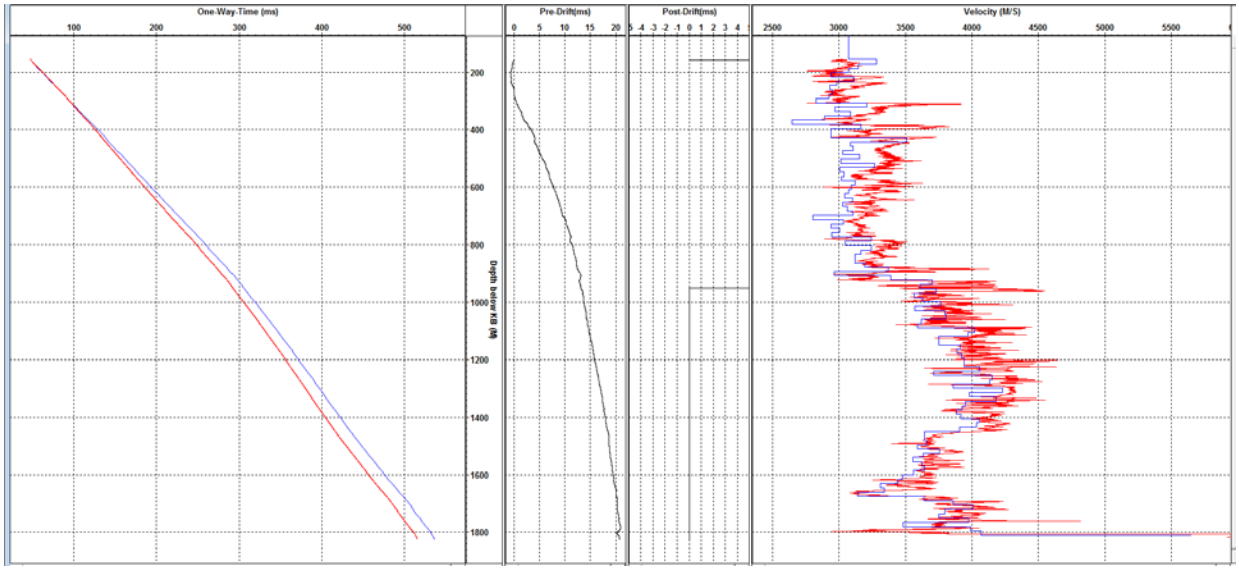

Figure 11 Sonic log before calibration: blue-VSP velocities, red – sonic log velocities

The sonic log calibrated this way can now be used for a synthetic seismogram generation that will tie the surface seismic.

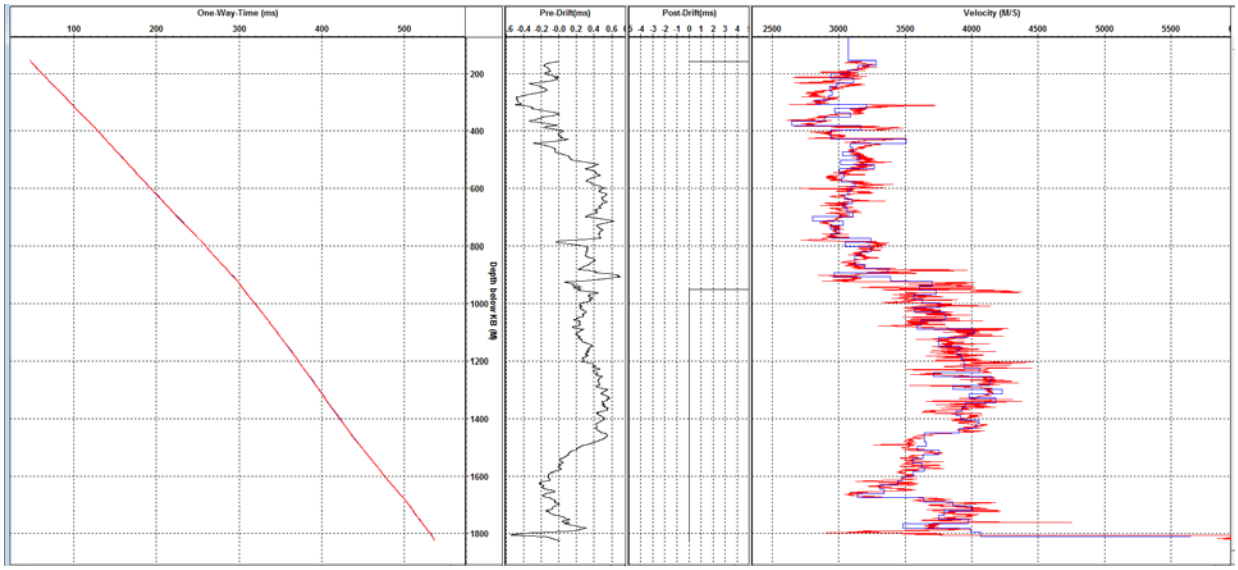

Figure 12 Sonic log after calibration: blue-VSP velocities, red – sonic log velocities

Step 5 – Wave-field separation

Wave-field separation was achieved using a 15 traces median filter along the first breaks to separate the down-going P wave-field (Figure 13). The median filter removed any up-going energy and random noise leaving just the down-going energy. Once we have the down-going only data file we can subtract that from the "total" wave-field that includes both the up and down-going data. The result of the subtraction is a file with the up-going data plus noise. The resultant up-going P wave-field is shown in Figure 14.

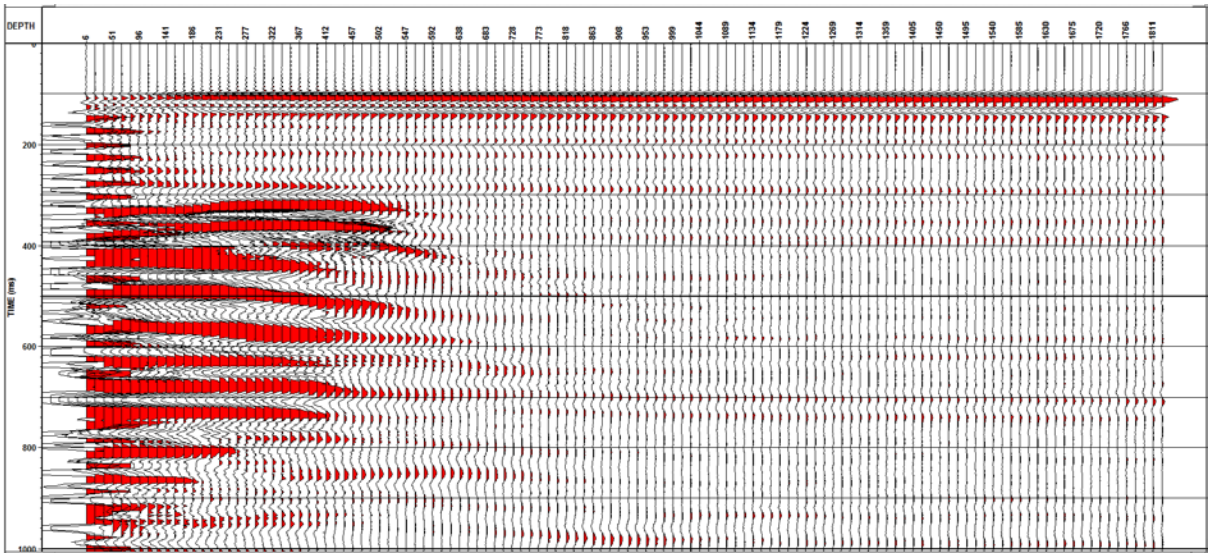

Figure 13 Downgoing P wavefield – flattened at 100ms – vertical component

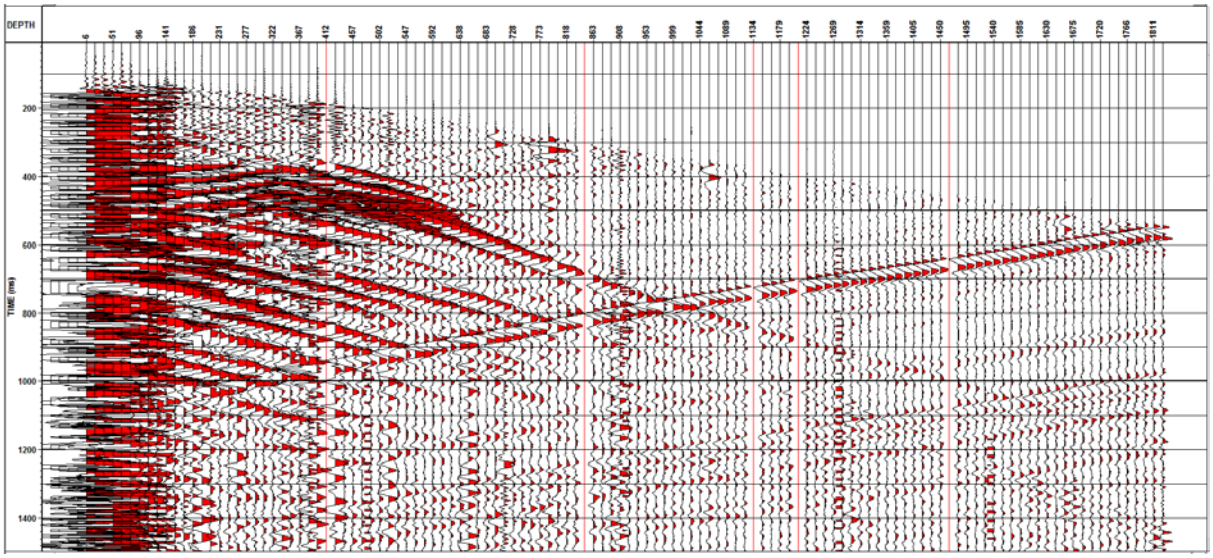

Figure 14 Upgoing P wavefield – vertical component

Step 6 – Deterministic Deconvolution – The down-going P wave-field was used to calculate a deconvolution operator (180ms window). The input down-going only wave form was wave shaped to a zero phase band limited output. The down-going only file contains all the earth filtering effects of the well length. As we have recorded the earth filtering effects we can determine the wave shaping operator "deterministically" rather than the statistical approach used in surface seismic processing allowing for a known zero phase result. Below are shown the deconvolved down-going P wave-field (Figure 16) and deconvolved up-going P wave-field (Figure 15).

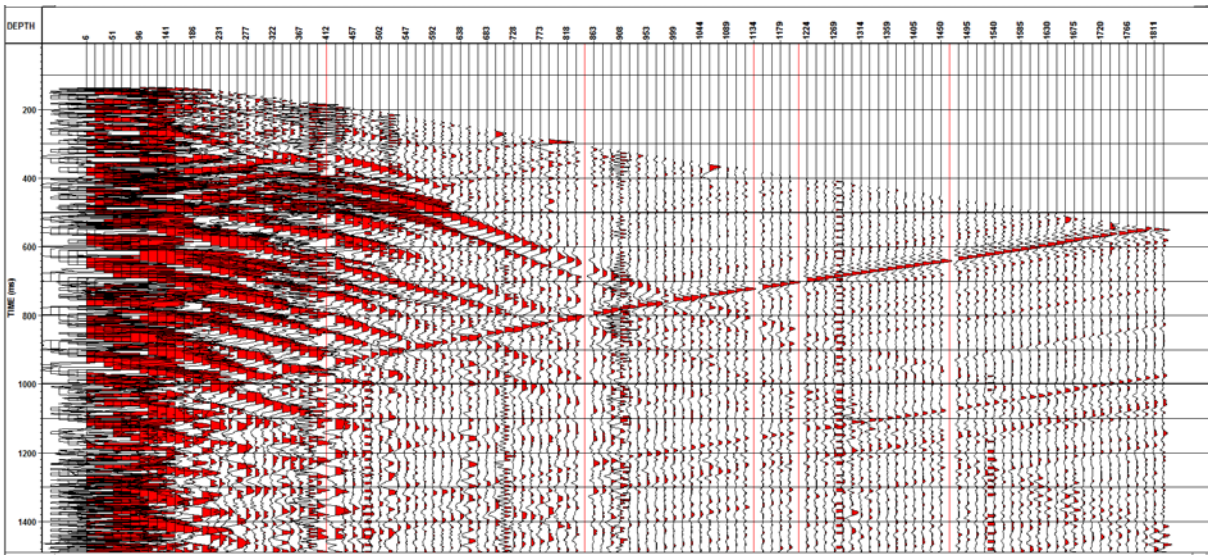

Figure 15 Upgoing P wavefield after deconvolution

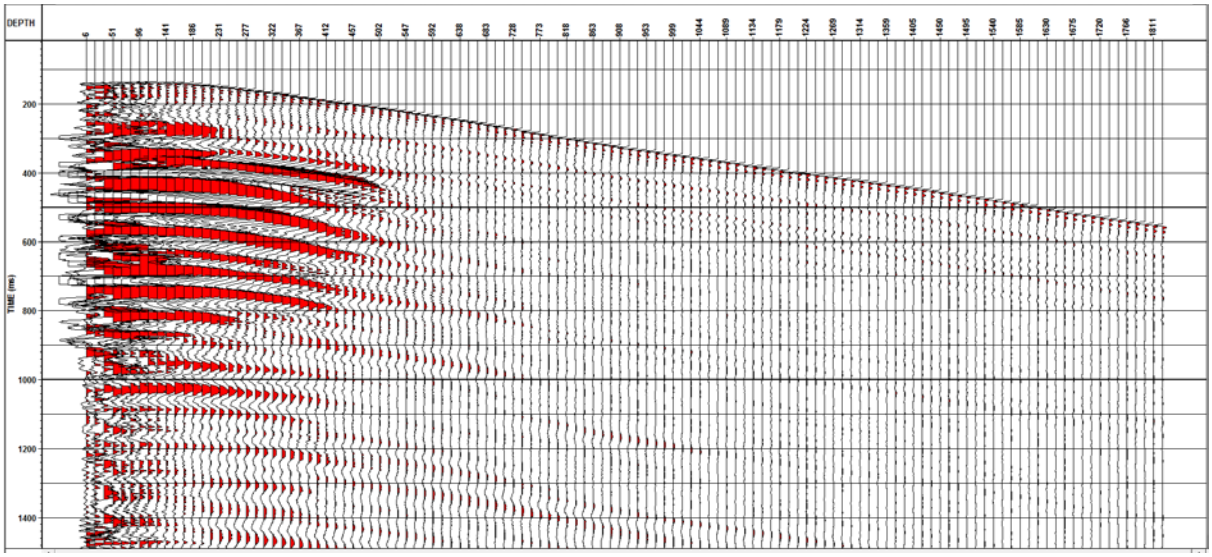

Figure 16 Downgoing P wavefield after deconvolution

Step 7 – NMO corrections and data in two-way-time – after nmo corrections each trace was shifted in time with an amount equal to the first break pick of that trace.

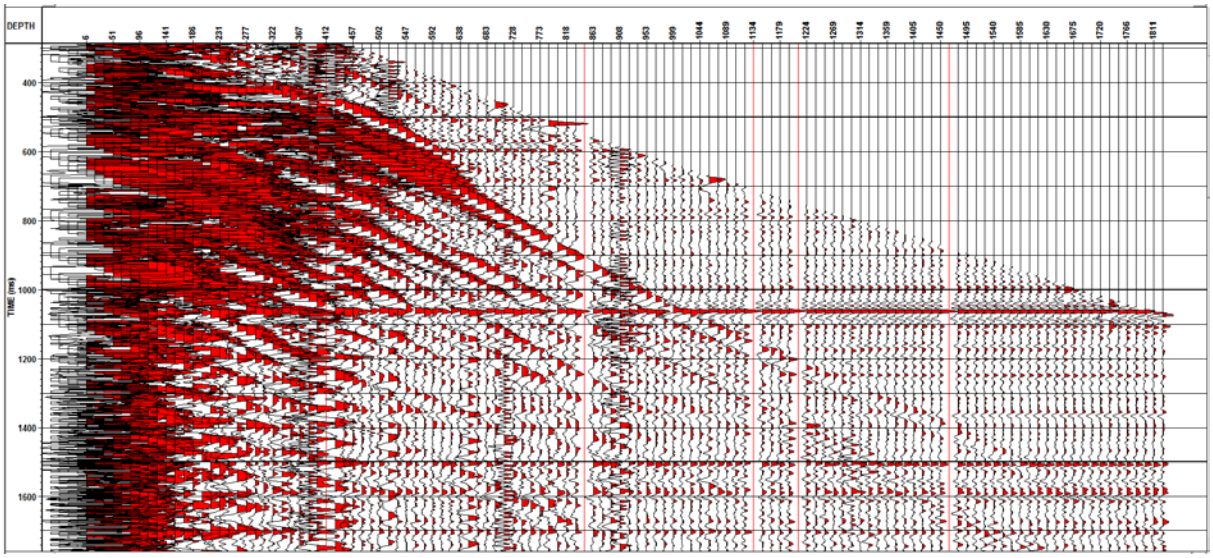

Figure 17 Upgoing P in TWT

Step 8 – Enhancement and edit – a 9 traces median was applied and noisy portions of the traces were removed

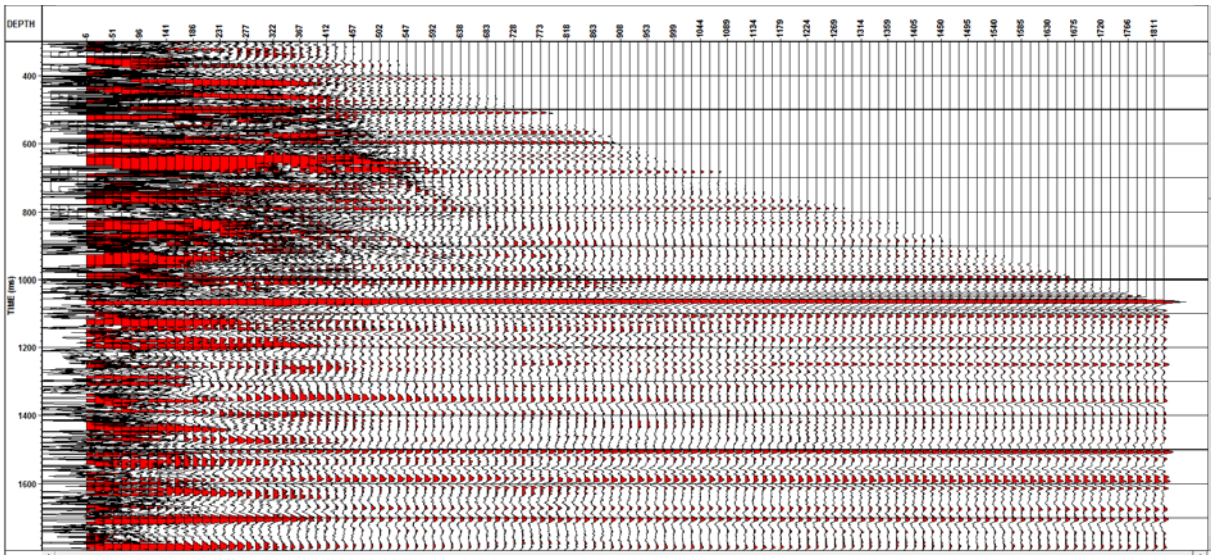

Figure 18 Data after enhancement

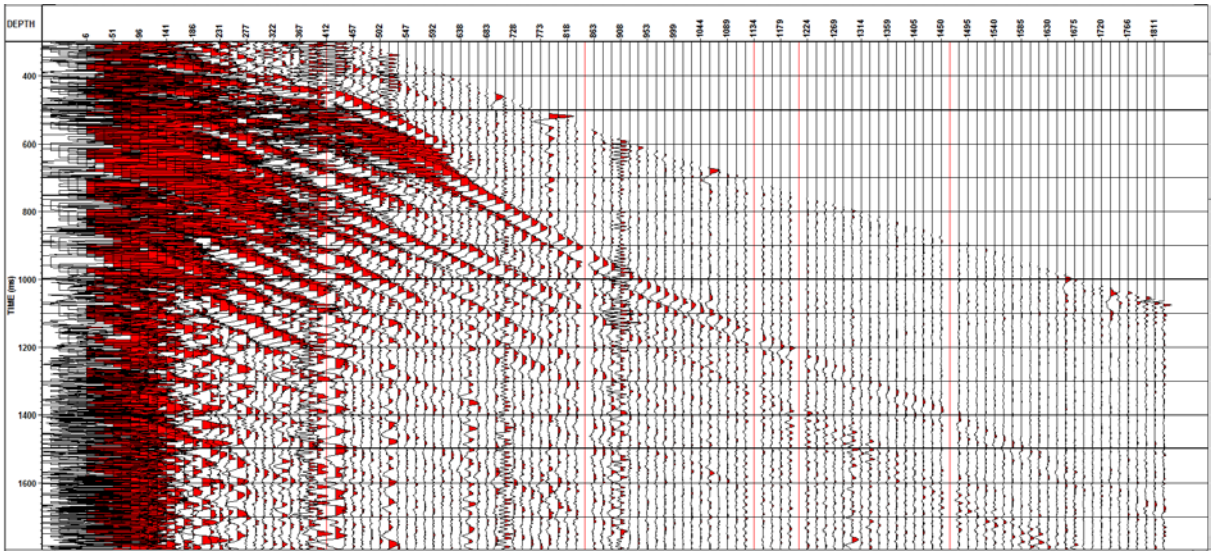

Figure 19 Residual wave-field

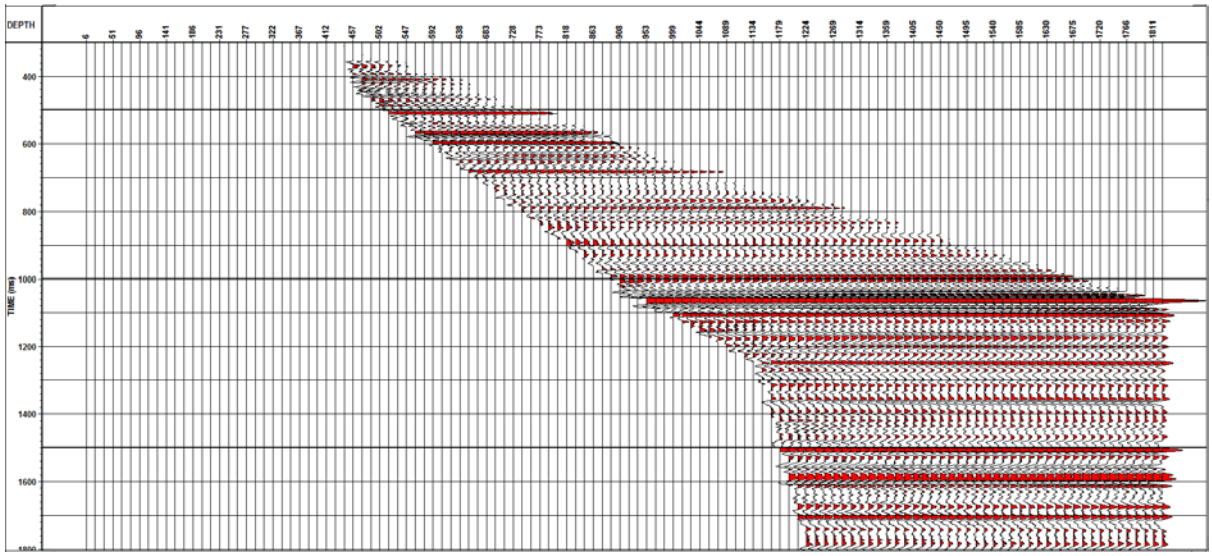

Figure 20 Data after edit

Step 9 – Corridor stack – After the enhancement of two way time data an outside window of data is stacked within a 100ms corridor.

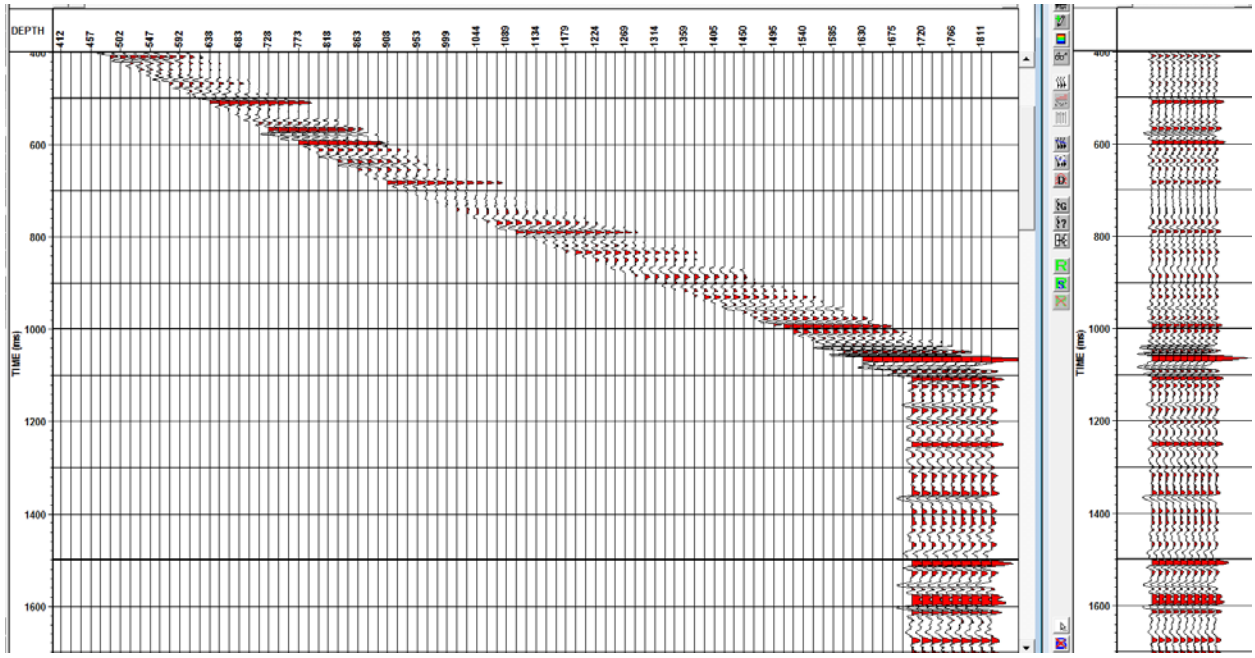

Figure 21 Corridor of data used in stack (left) and corridor stack (right)

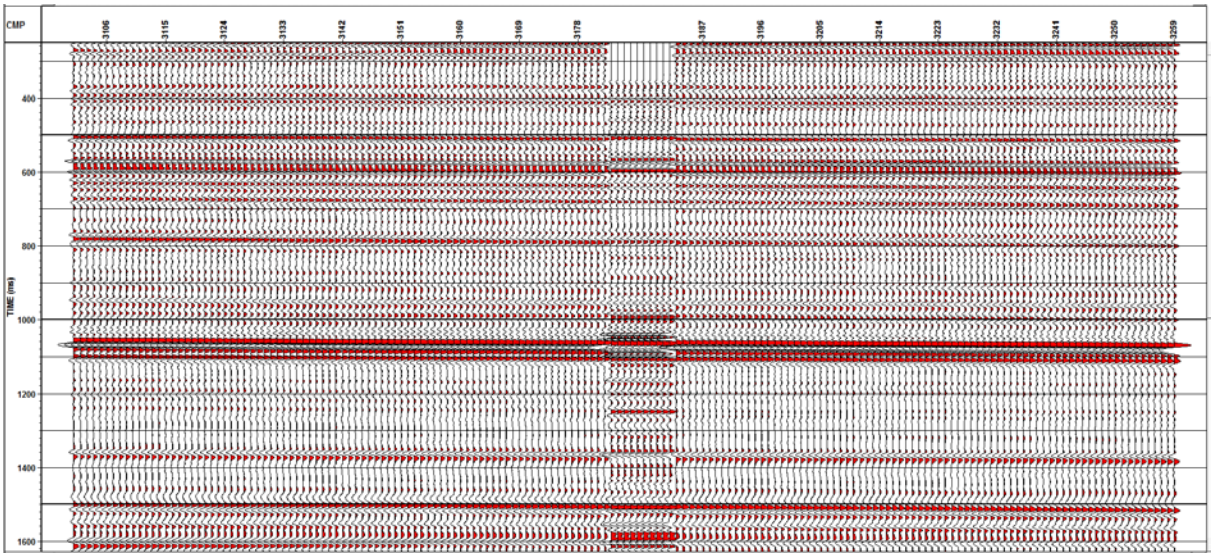

Figure 22 Seismic section TUL20 with corridor stack

Step 10 – VSP-CDP mapping – The shot-point used in the zero offset processing is quite far from the well and an image of the subsurface was also calculated.

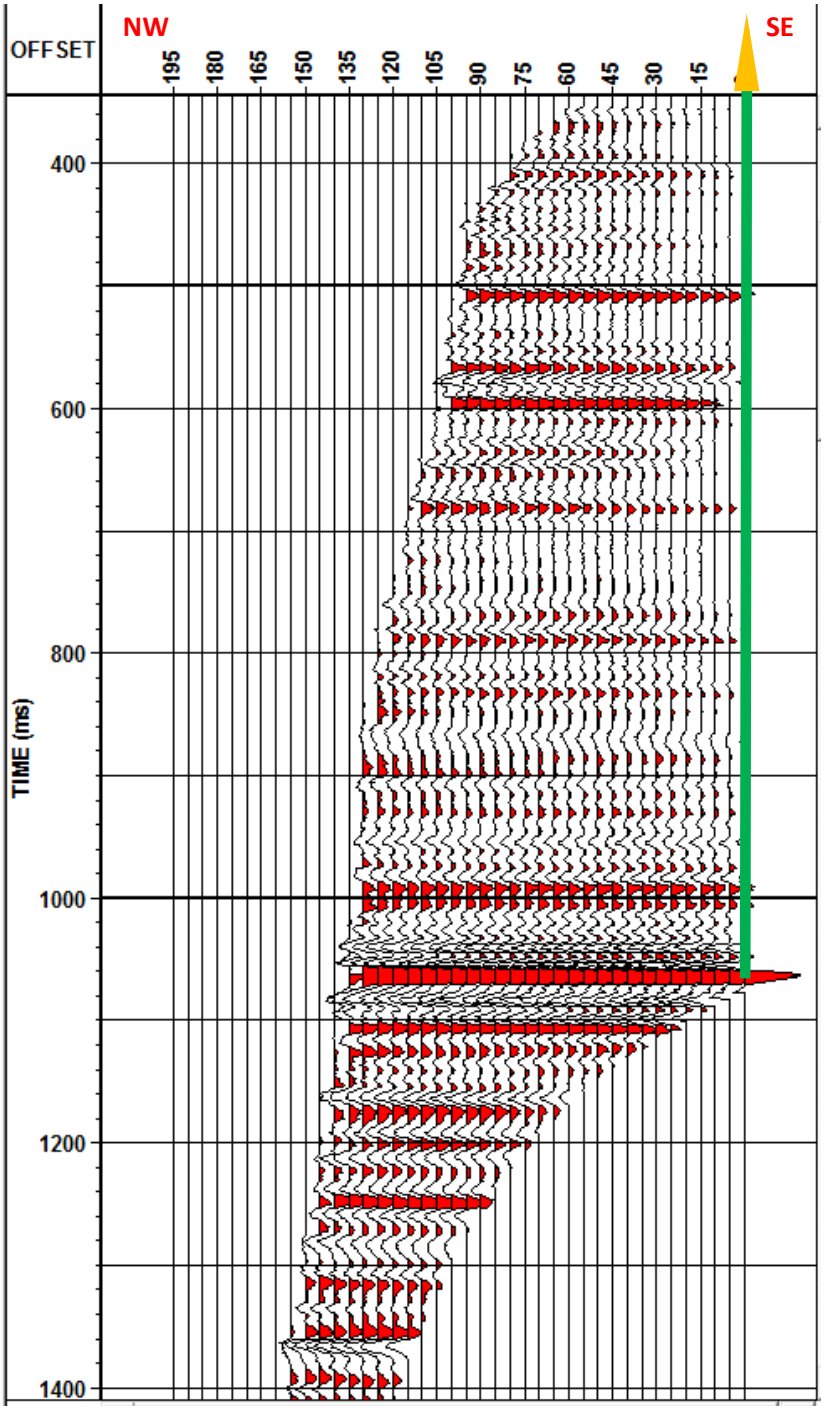

Figure 23 VSP - CDP map - 5m between traces

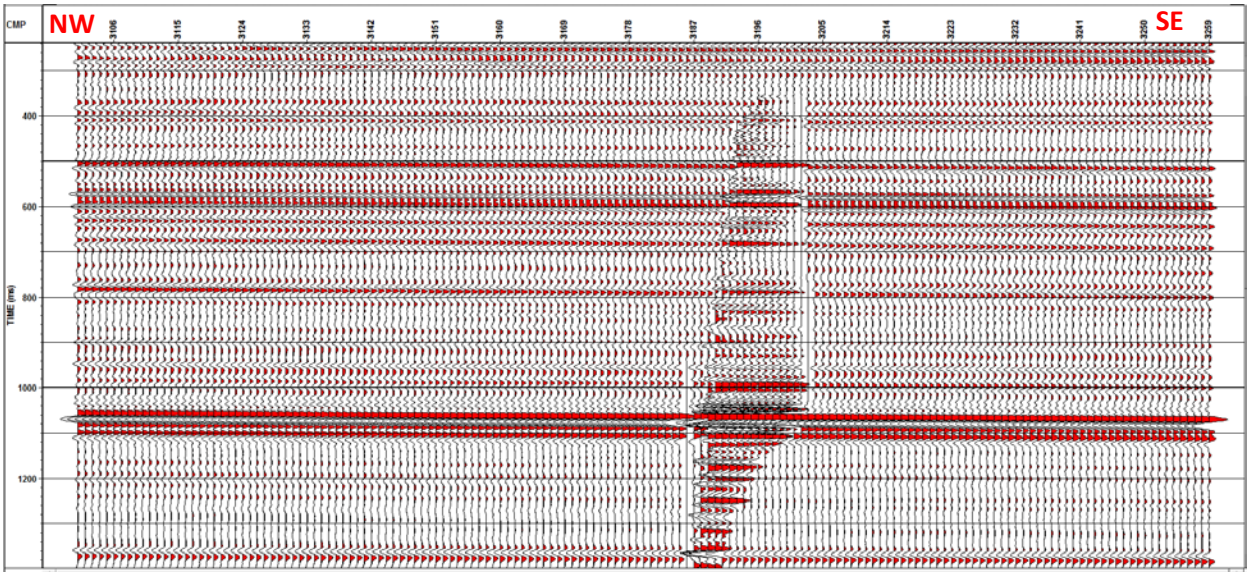

Figure 24 Seismic section TUL20 with vsp-cdp map (10m between traces) inserted

Walkaway VSP – PP processing

Only the vertical component was used in the walk-away processing. Maximum offset used was 1378m. To illustrate the processing steps, 3 shot-points (239 – 1378m offset; 206 – 781m offset and 168 – 435m offset) of the walk-away line are shown below. Total number of shot-points was 139.

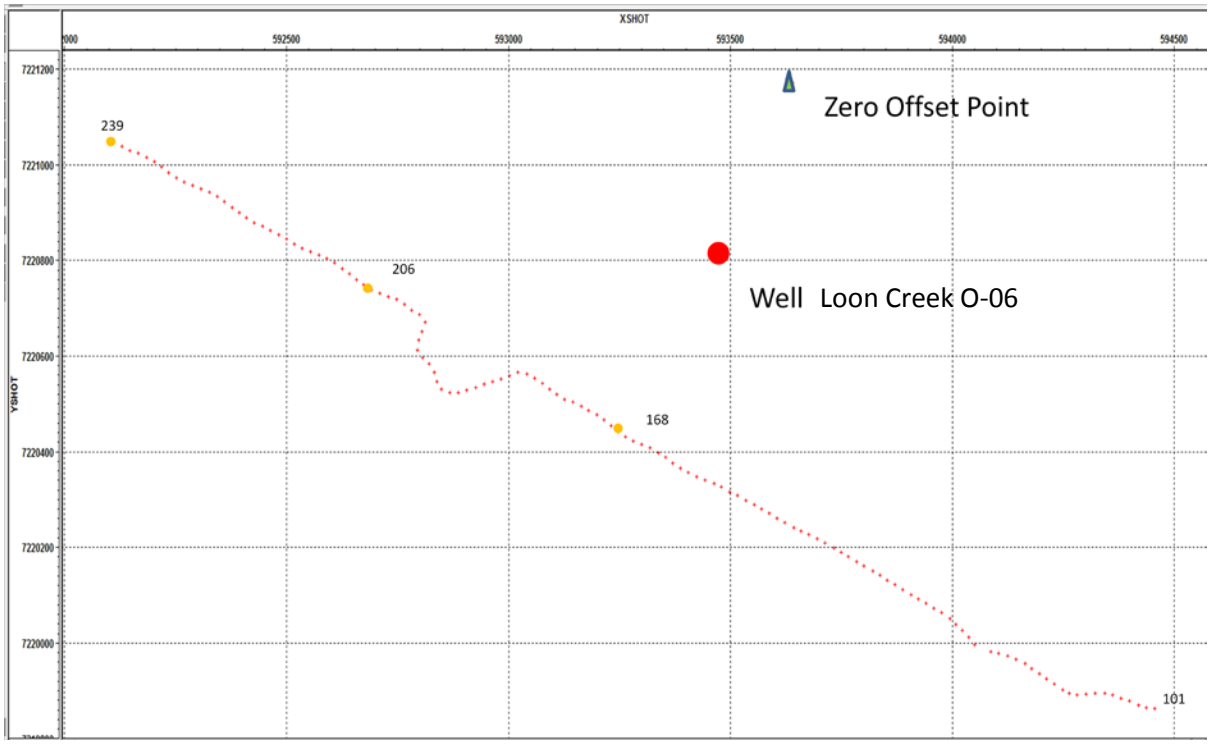

Figure 25 Basemap

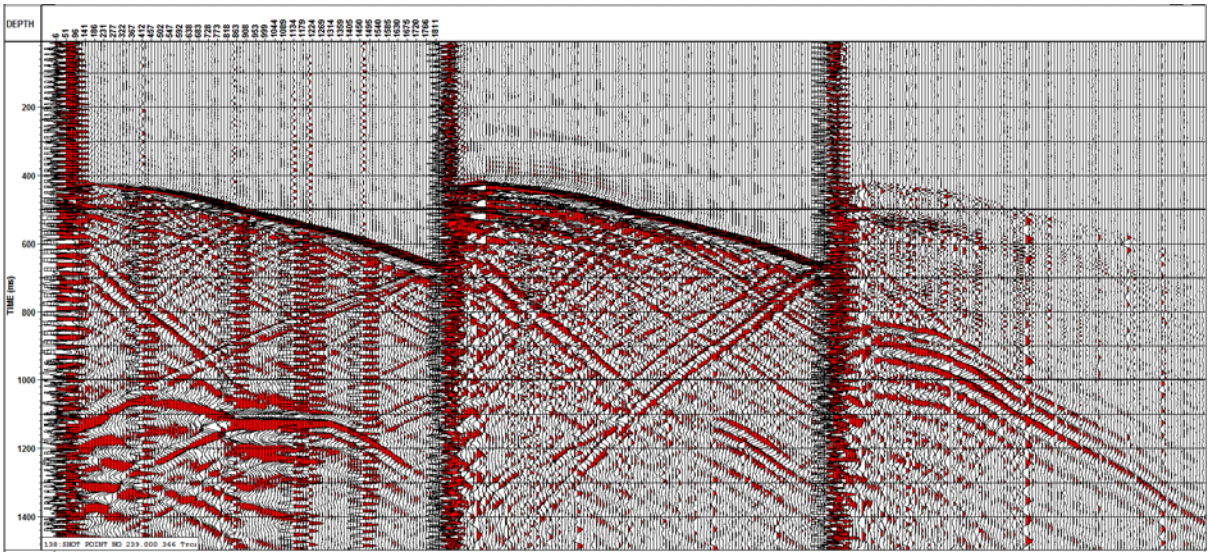

Figure 26 Shot-point 239 – raw data after rotation – Z (left), Hmax (middle), Hmin (right) components – field recorded time

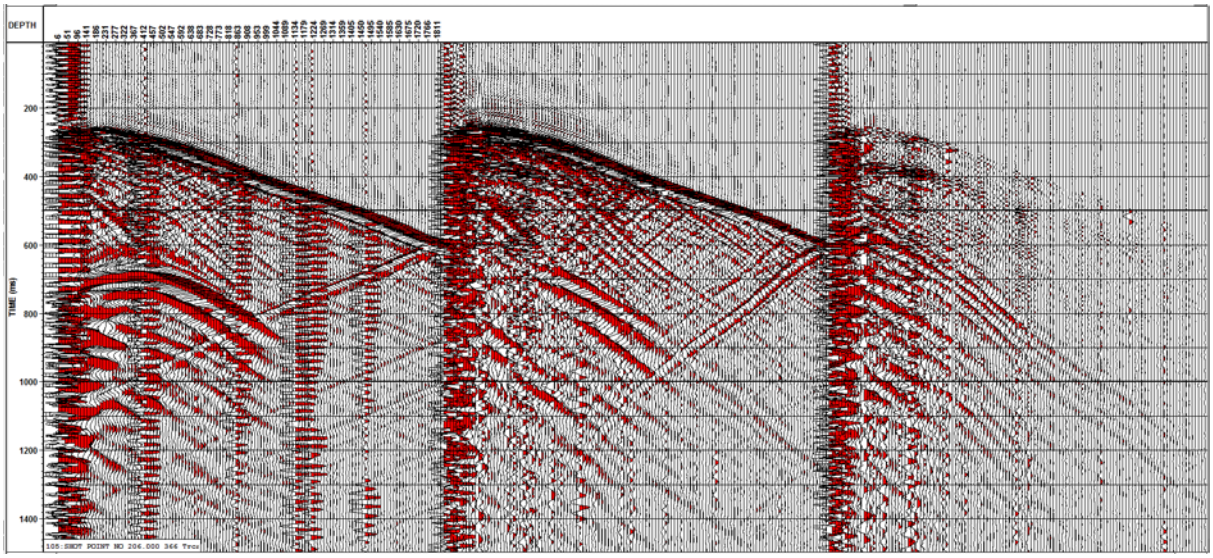

Figure 27 Shotpoint 206 – raw data after rotation – Z (left), Hmax (middle), Hmin (right) components – field recorded time

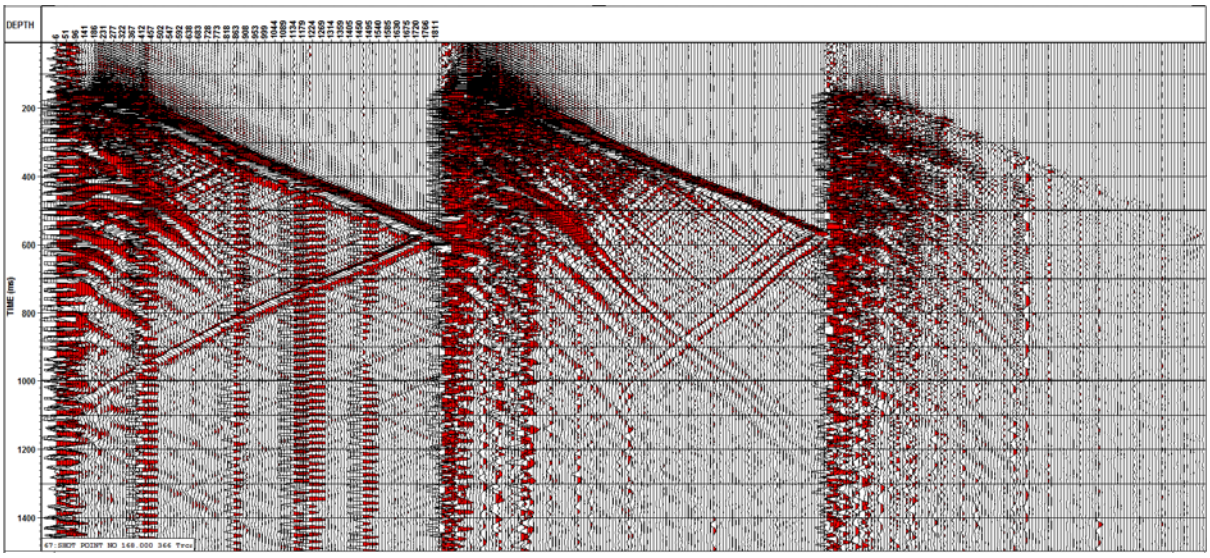

Figure 28 Shotpoint 168 – raw data after rotation – Z (left), Hmax (middle), Hmin (right) components – field recorded time

Type of waves observed

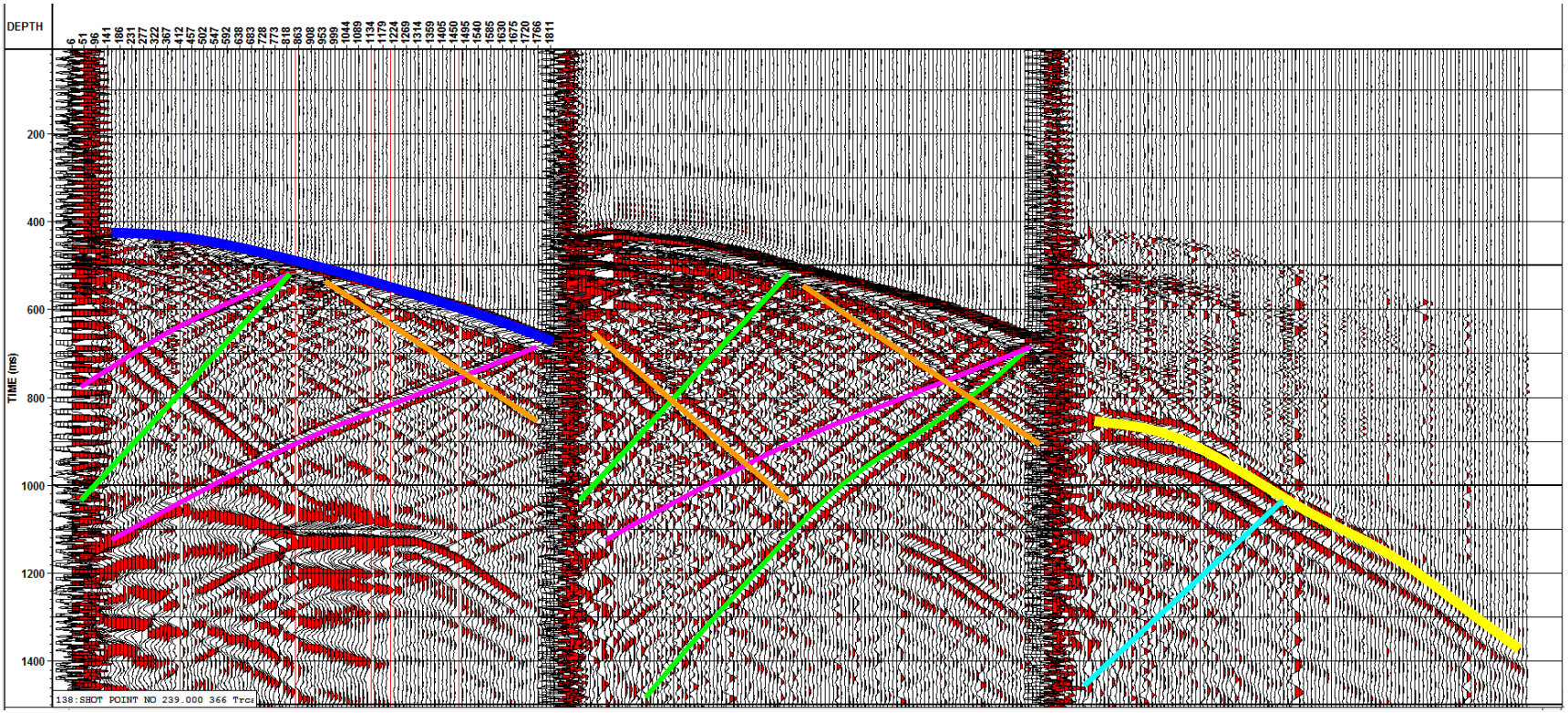

Figure 29 Shot-point 239 – raw data after rotation – Z (left), Hmax (middle), Hmin (right) components – field recorded time

	Down-going P		Up-going PS
	Down-going S		Down-going PS
	Up-going PP		Up-going SS

Processing steps – vertical component

Step 1 – Geometry – source and well coordinates, source depths and receiver depths were applied to the data

Step 2 – Source elevation datum corrections – Data was shifted to 257.6m (KB) datum using 3200m/sec replacement velocity.

Step 3 – First breaks picking – Transit times were picked on the vertical component.

Step 4 – Amplitude correction – A spherical divergence correction (T power 1.5) was applied

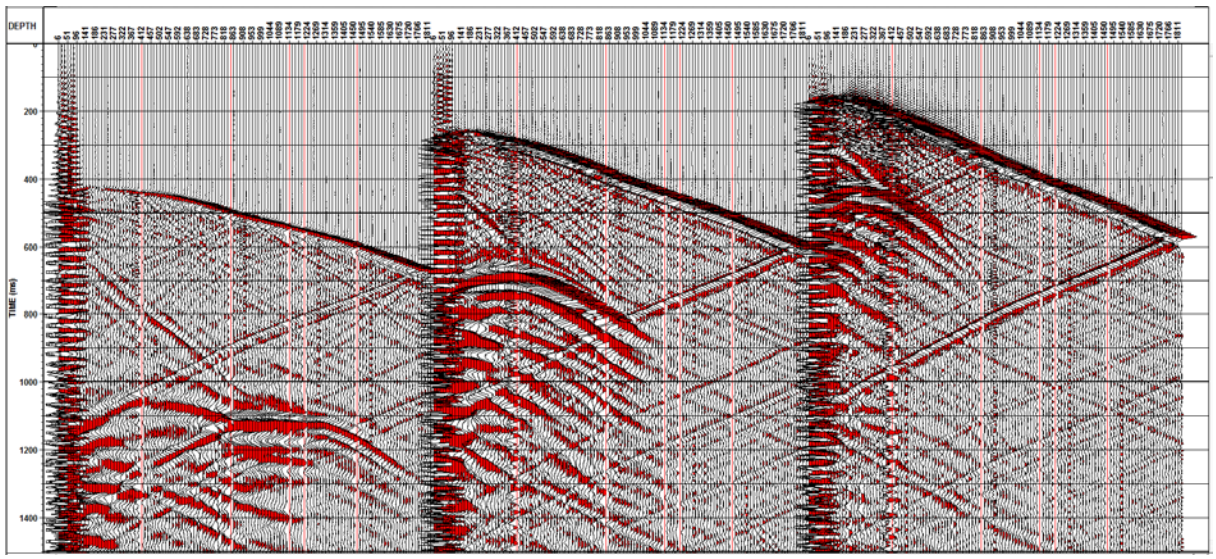

Figure 30 Shotpoint 239(left), 206(middle and 168(right) – vertical component – raw data corrected for spherical divergence – field recorded time – datum KB

Step 5 – Wavefield separation

Wavefield separation was achieved using a 15 traces median filter along the first breaks to separate the downgoing P wavefield (Figure 31). The median filter removed any upgoing energy and random noise leaving just the downgoing energy. Once we have the downgoing only data file we can subtract that from the "total" wavefield that includes both the up and downgoing data. The result of the subtraction is a file with the upgoing data plus noise. The resultant upgoing P wavefield is shown in (Figure 32).

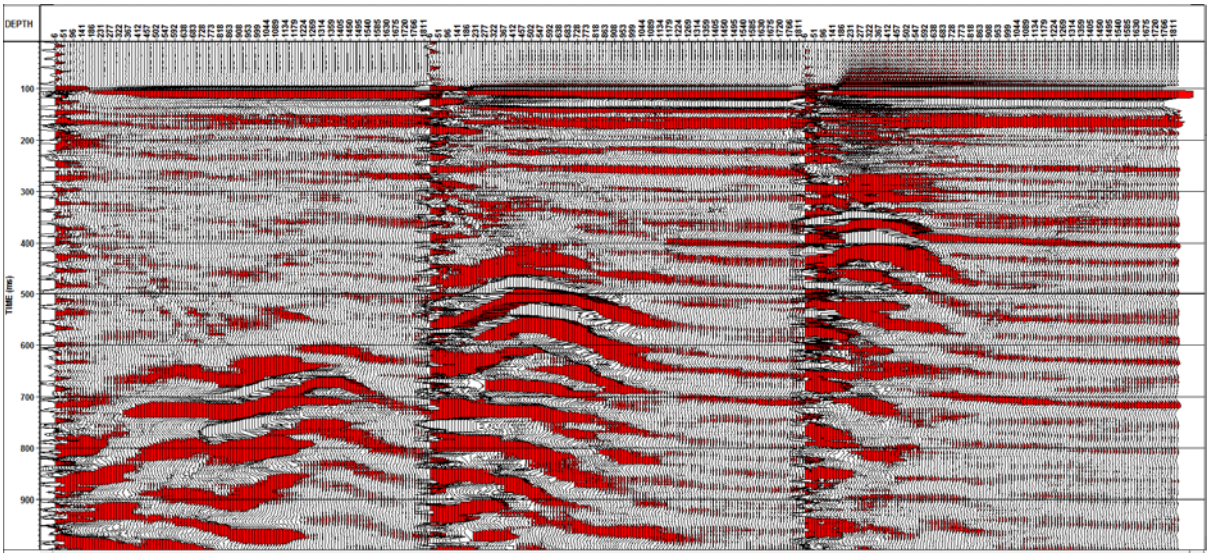

Figure 31 Shotpoint 239(left), 206(middle) and 168(right) – vertical component – wave-field separation - down-going P – data flattened at 100ms

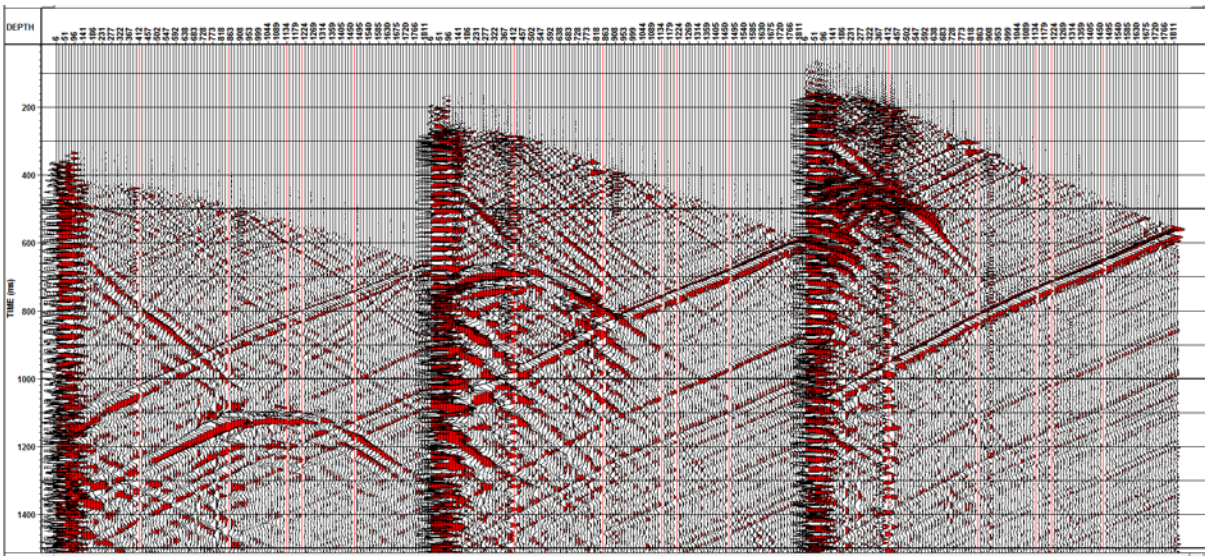

Figure 32 Shot-point 239(left), 206(middle) and 168(right) – vertical component – wave-field separation - data after down-going P removal – field recorded time

Step 6 – Deterministic Deconvolution – The down-going P wave-field was used to calculate a deconvolution operator (180ms window). A single trace (down-going P wave-field of the deepest geophone) was used to calculate the deconvolution operator for all the geophones (one deconvolution operator for each shot-point). The input down-going only wave form was wave shaped to a zero phase band limited output. The down-going only file contains all the earth filtering effects of the well length. As we have recorded the earth filtering effects we can determine the wave shaping operator "deterministically" rather than the statistical approach used in surface seismic processing allowing for a known zero phase result. All frequencies are included in the deconvolution. Below is shown the deconvolved down-going P wave-field (Figure 34) and deconvolved up-going P (Figure 33)

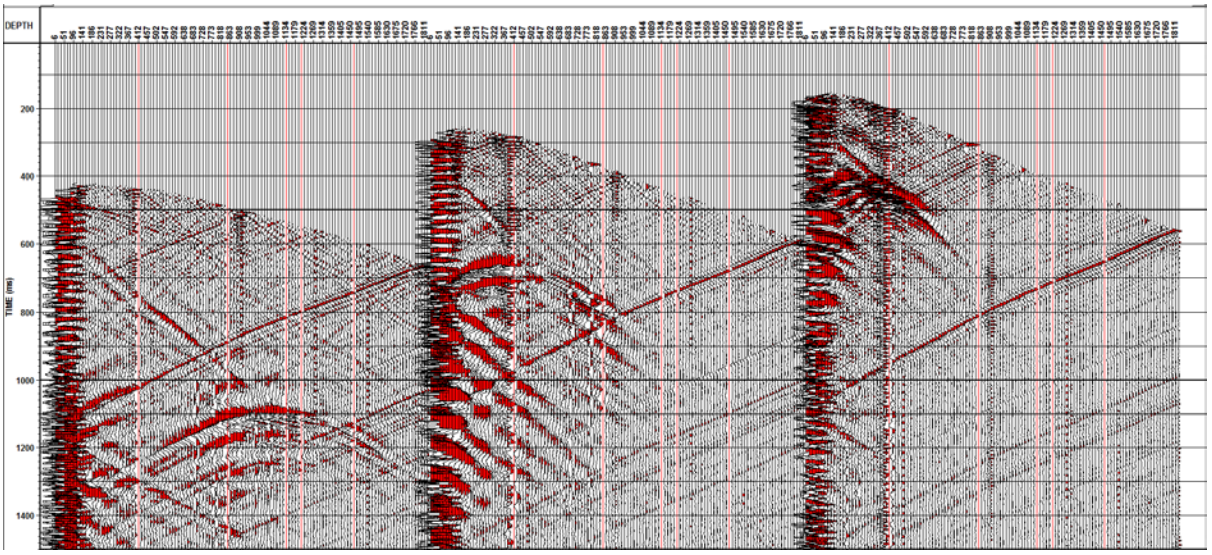

Figure 33 Shot-point 239(left), 206(middle) and 168(right) – vertical component – up-going P data after deconvolution – field recorded time

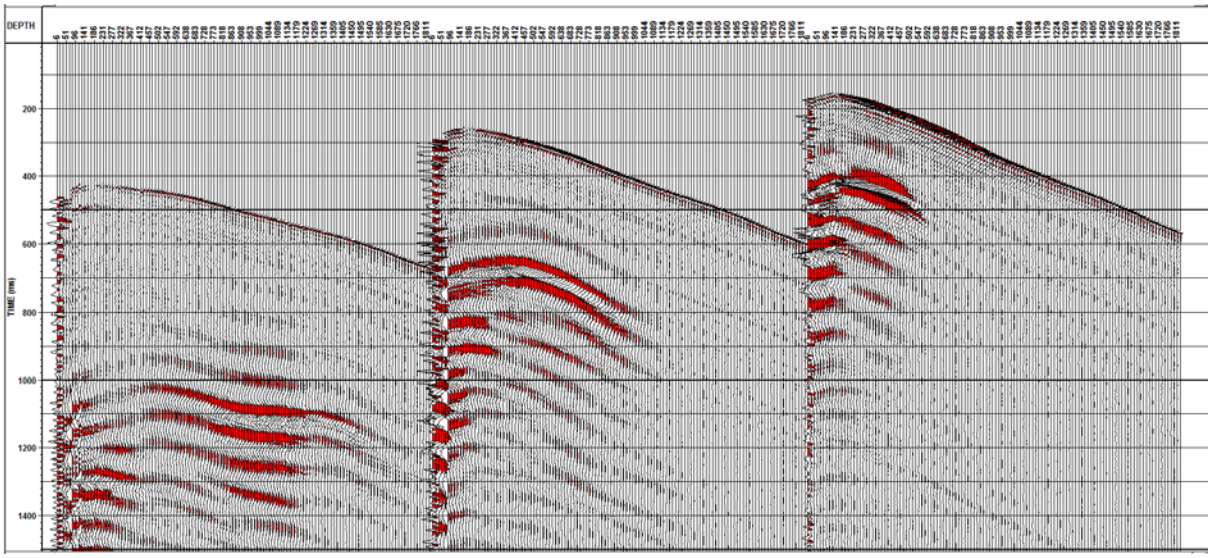

Figure 34 Shot-point 239(left), 206(middle) and 168(right) – vertical component – down-going P data after deconvolution – field recorded time

Step 7 – FK filter and edit – After deconvolution the up-going (Figure 33) wave-field is filtered in FK domain to remove all down-going waves left. Also the first 6 levels were muted out (Figure 35).

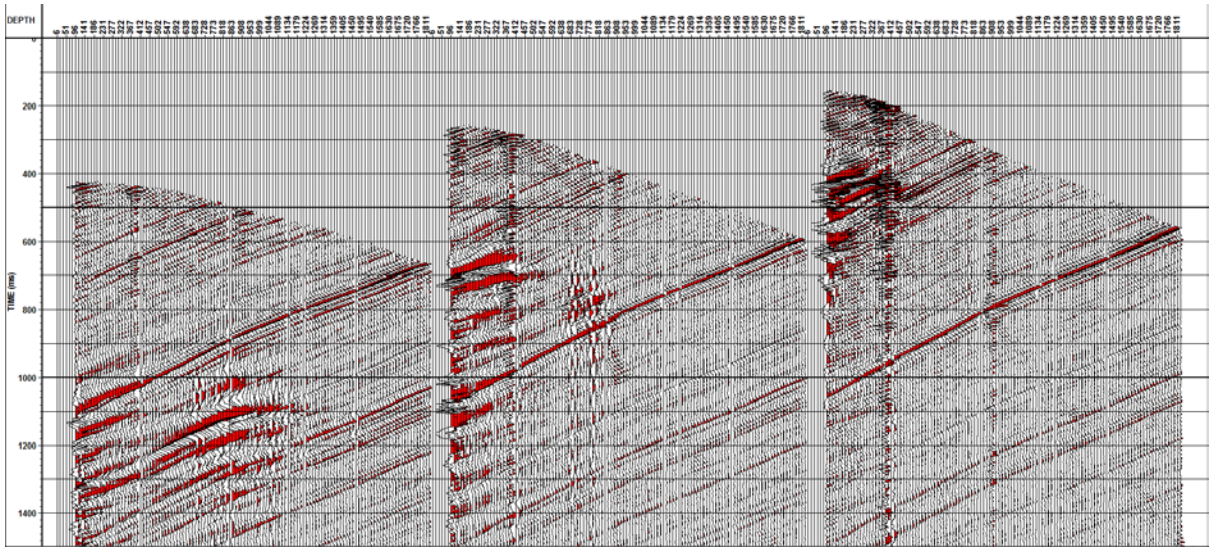

Figure 35 Shot-point 239(left), 206(middle) and 168(right) – vertical component – up-going P data after FK filtering – field recorded time

Step 8 – NMO corrections and two way PP time – After FK filtering the up-going wave-field is NMO corrected with Zero offset velocities and transformed into two way PP time (Figure 36).

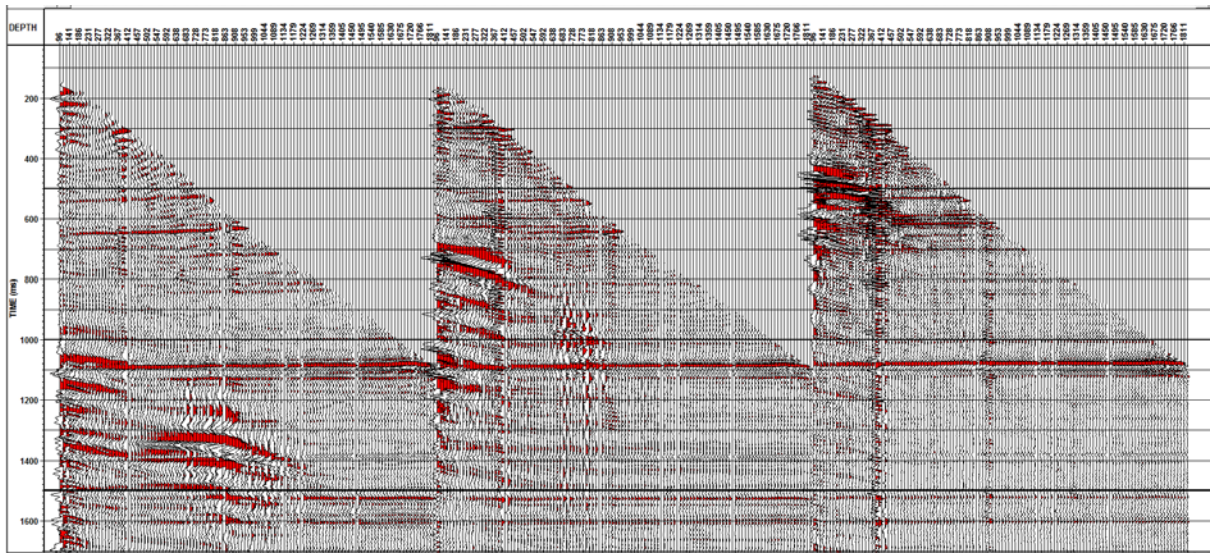

Figure 36 Shot-point 239(left), 206(middle) and 168(right) – vertical component – up-going P data after NMO corrections – two way PP time

Step 9 – Enhancement – A 7 traces median filter was used for enhancement.

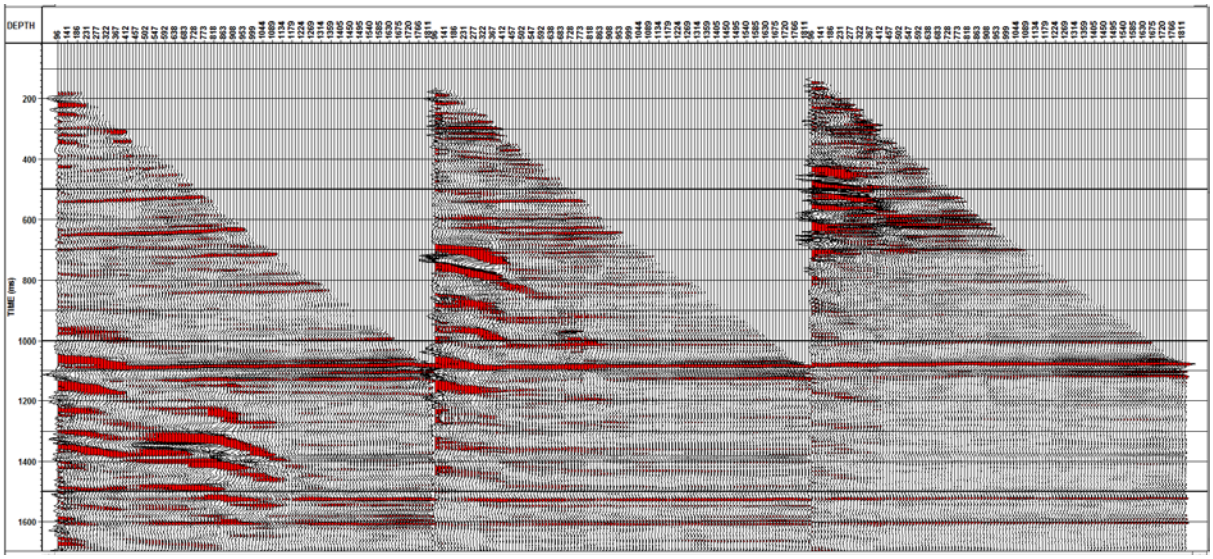

Figure 37 Shot-point 239(left), 206(middle) and 168(right) – vertical component – up-going P data after enhancement (7 traces median) – two way PP time

Data shown in Figure 37 is the final step of the processing before vsp-cdp mapping.

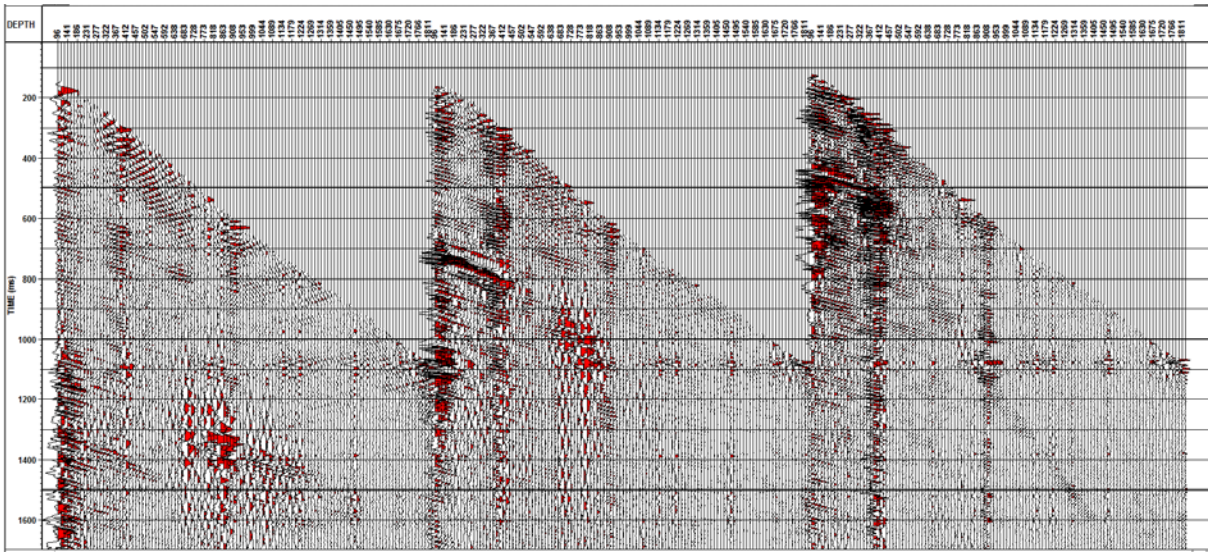

Figure 38 Shot-point 239(left), 206(middle) and 168(right) – vertical component – residual wave-field – two way PP time

Step 10 – VSP – CDP mapping – For each shot-point a vsp-cdp map (5m between traces) was generated. The spatial distribution is shown in Figure 39. If we are projecting all the data on a vertical plane parallel with the walk-away source line (Figure 39) the result will be as in Figure 40.

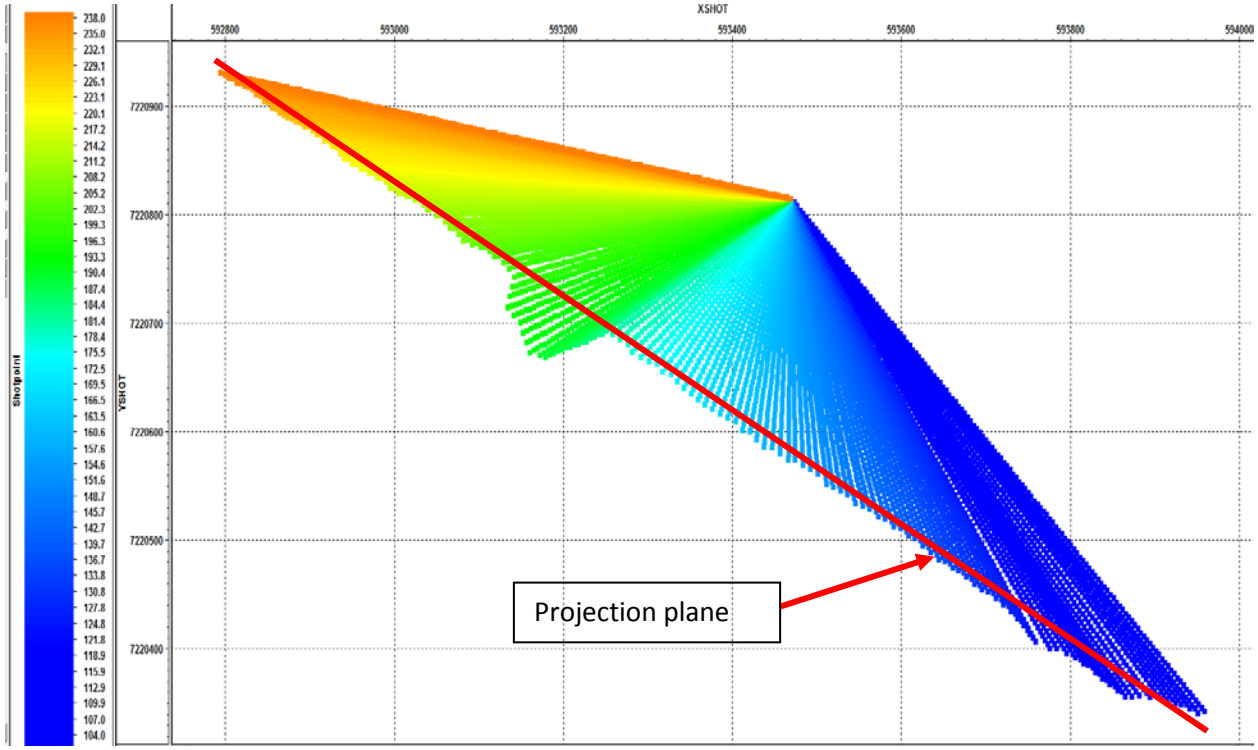

Figure 39 Spatial distribution of the subsurface reflection points after vsp-cdp mapping

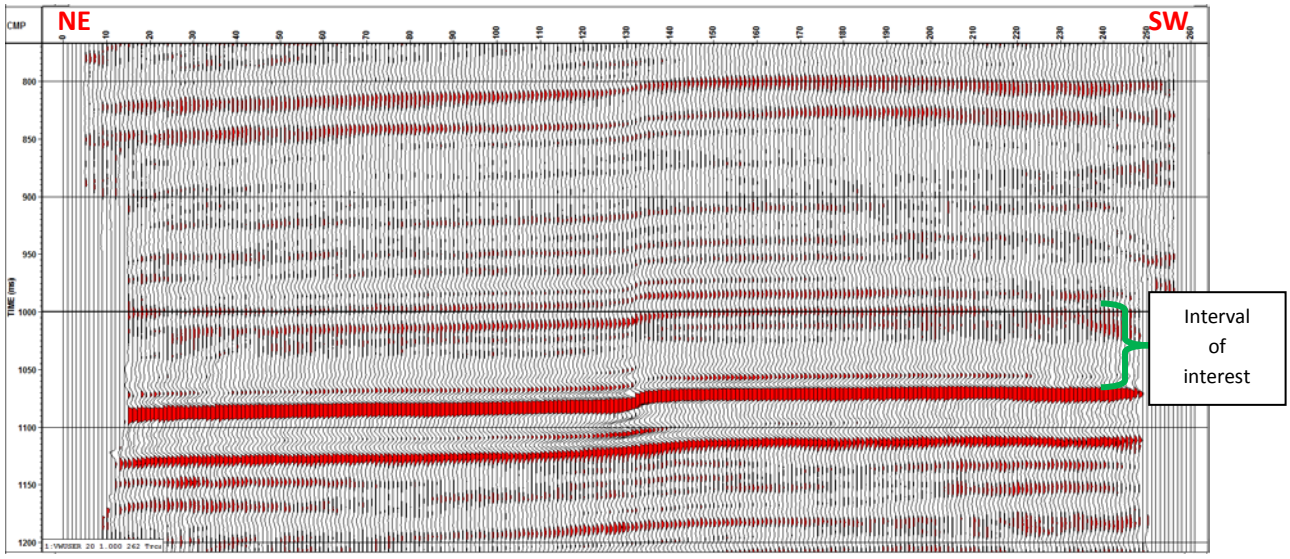

Figure 40 VSP-CDP map with all data stacked

Looking at Figure 40 we can see a problem: the shift of the data in the middle of the profile. This shift is not real. The explanation of this shift is that we are stacking data from a tri-dimensional structure (the

reflectors are not horizontal). To obtain a correct image we have to stack a narrow band of data. The next step in the processing was to select a narrow band of data, re-binning and stacking.

Step 11 – Re-binning – A narrow band of data was selected as in Figure 41.

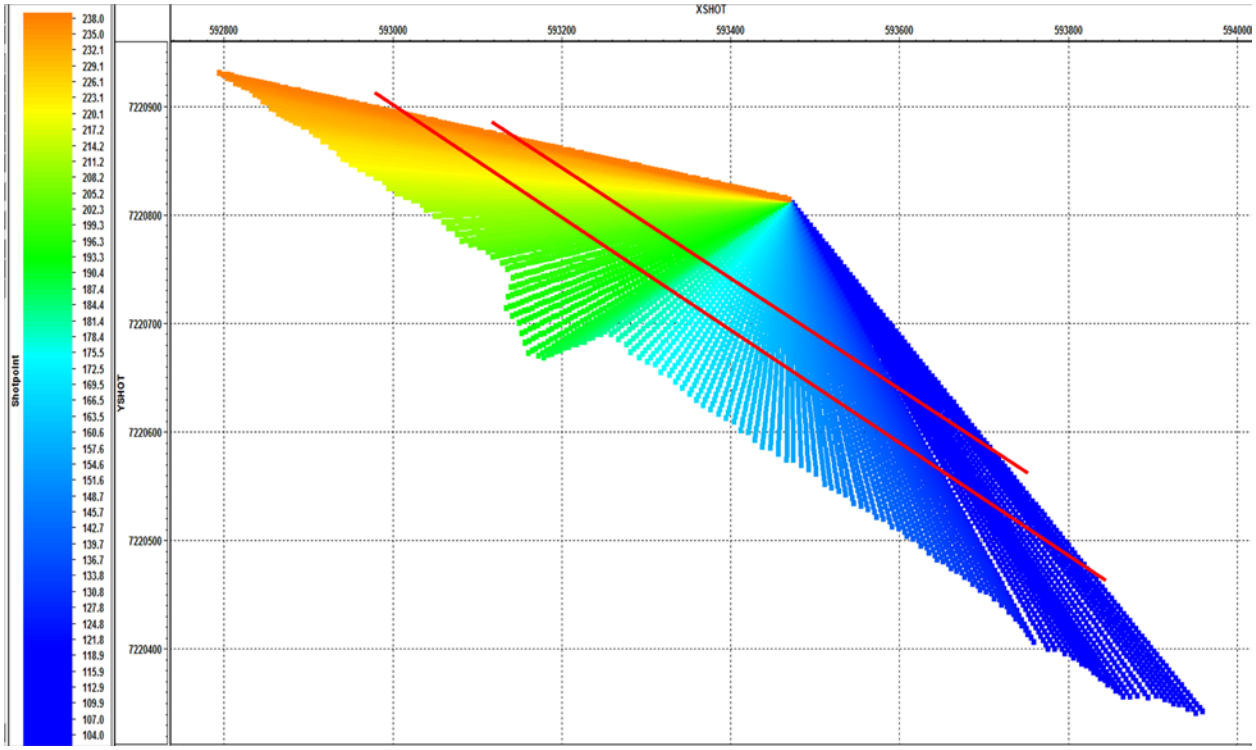

Figure 41 Selected data for re-binning and stacking

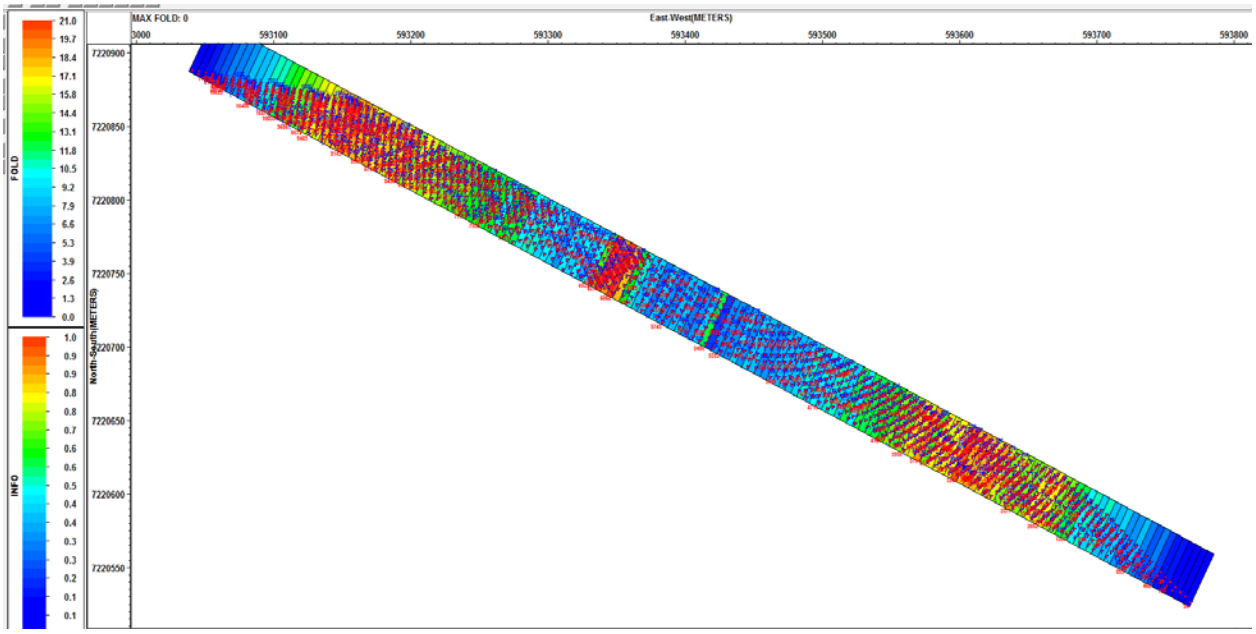

Figure 42 Re-binning of the data

Re-binning cell was 5m wide and 40m long. Maximum fold achieved was 21.

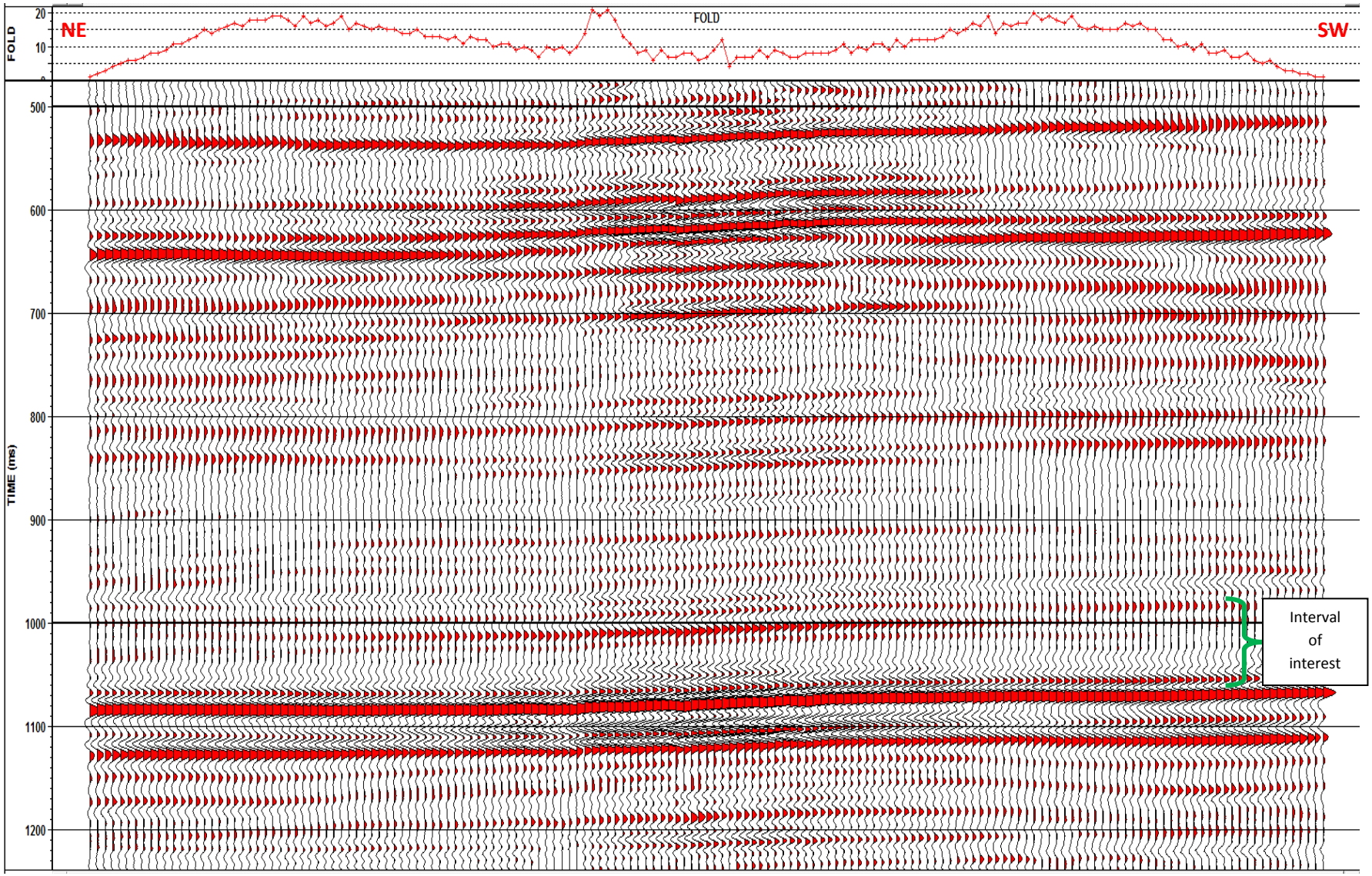

Figure 43 Walk-away line after re-binning and stacking

RESERVOIR IMAGING

ConocoPhillips Canada

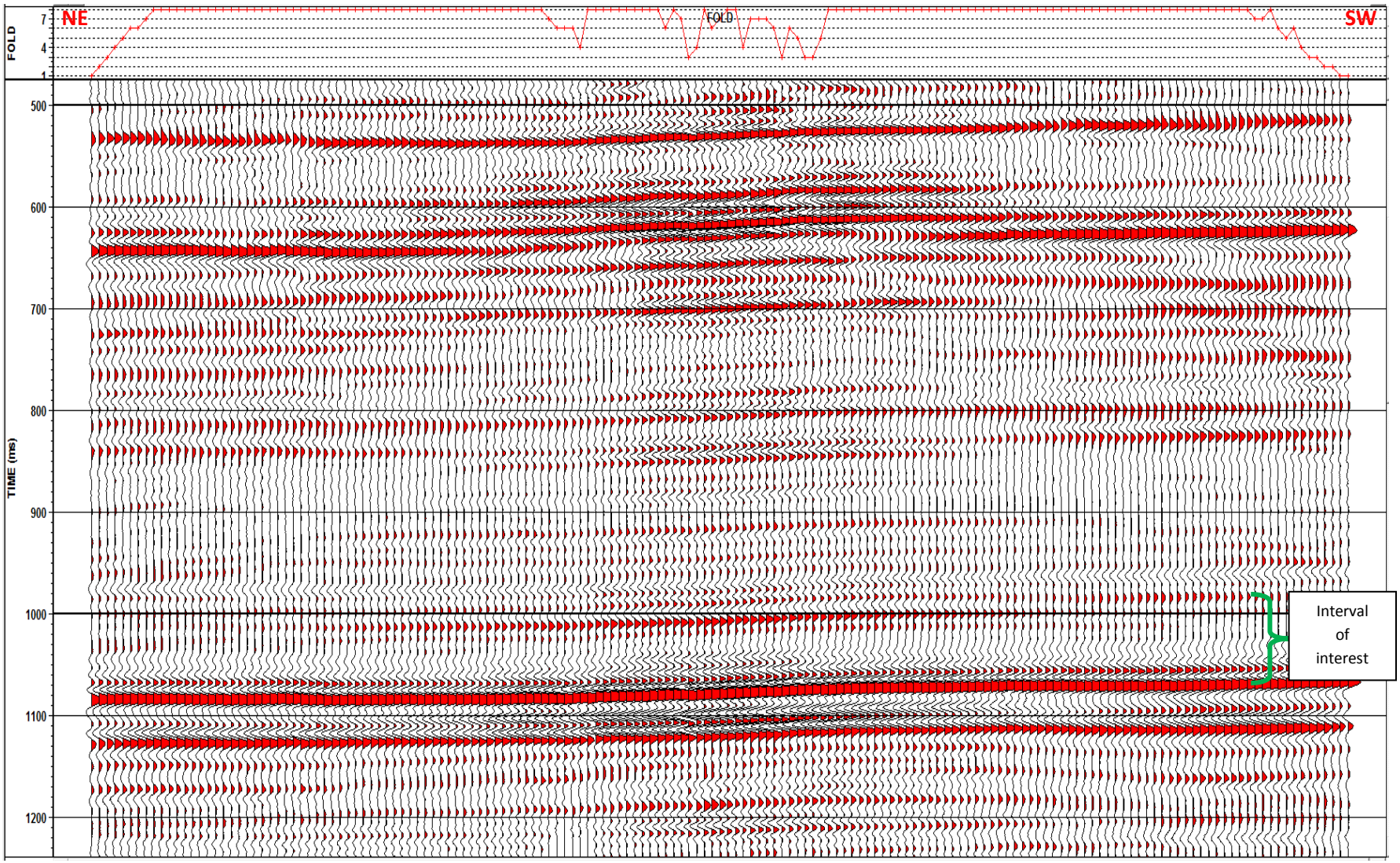

Figure 44 Walk-away line after re-binning, stacking and fold reduction (fold 8)

RESERVOIR IMAGING

ConocoPhillips Canada

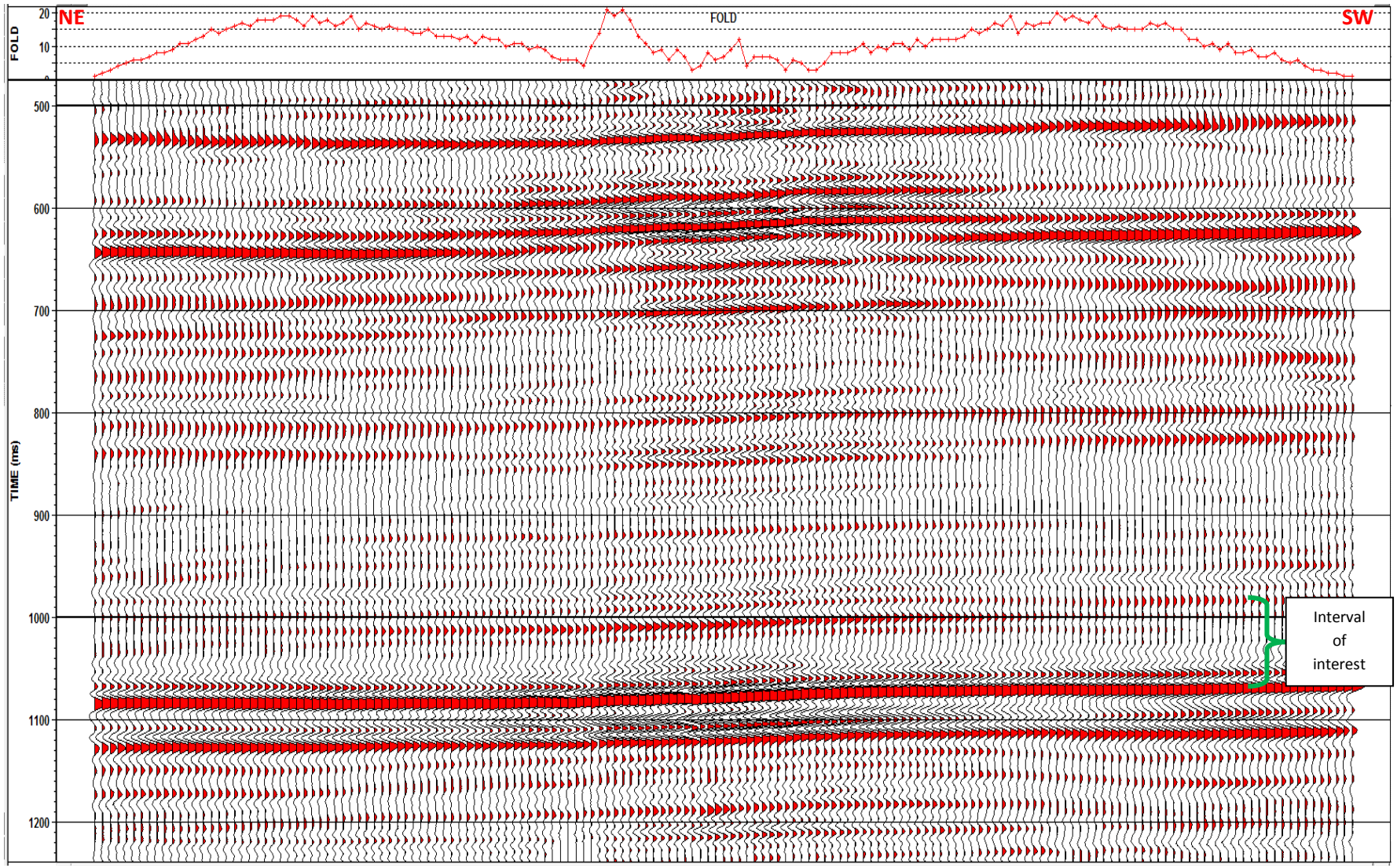

Figure 45 Walk-away line after re-binning, stacking and editing

RESERVOIR IMAGING

ConocoPhillips Canada

The final images of the walk-away:

- Figure 43 – walk-away line after re-binning and stacking
- Figure 44 – walk-away line after re-binning, fold reduction and stacking
- Figure 45 – walk-away line after re-binning, editing and stacking

The fold reduction was performed to make all traces comparable from signal/noise ratio point of view and consisted of manually deleting traces in CMP gathers (before stacking).

The editing consisted of deleting certain traces in CMP gathers that were causing discontinuities of the stacked traces.

Final observations

All the processing performed on the data is rigorous and in accord with the geometry of the survey and of the layers with one exception: due to software limitations the ray tracing that is performed in the vsp-cdp mapping was based on a velocity model with horizontal layers – this assumption is different from reality – the layers are dipping.

Disclaimer

In the processing and discussions of results based on the interpretation of the data seen Reservoir Imaging Ltd will give their clients the benefit of their best judgement however, Reservoir Imaging Ltd cannot and does not guarantee the accuracy or correctness of any interpretation or computation and shall not be liable for any loss, costs, damages or expenses incurred or sustained by the client resulting from any interpretation or computation made by Reservoir Imaging Ltd officers, agents or employees.